Contrib Mineral Petrol (2005) 150: 287–305
DOI 10.1007/s00410-005-0018-7

ORIGINAL PAPER

Xue-Ming Yang · David R. Lentz

Chemical composition of rock-forming minerals in gold-related granitoid intrusions, southwestern New Brunswick, Canada: implications for crystallization conditions, volatile exsolution, and fluorine-chlorine activity

Received: 31 January 2005 / Accepted: 1 July 2005 / Published online: 15 September 2005

Abstract Chemical composition of rock-forming minerals in Appalachian Siluro-Devonian granitoid intrusions, southwestern New Brunswick, was systematically determined by electron microprobe. The mineral chemical data together with petrographic examination was used to test magmatic equilibration and to constrain crystallization conditions, volatile exsolution, and fluorine-chlorine activity of fluids associated with these intrusions. Mineralogical distinction between Late Silurian to Early Devonian granodioritic to monzogranitic series (GMS) and Late Devonian granitic series (GS) rocks is evident, although both are subsolvus I-type to evolved I-type granitoids. Oxidized to reduced GMS rocks consist of quartz, plagioclase (An > 10), K-feldspar, biotite, apatite, titanite, zircon, monazite, ± hornblende, ± pyroxene, ± magnetite, ± ilmenite, and ± sulfide. GS rocks comprise quartz, K-feldspar, plagioclase (An < 10), mica group minerals, zircon, monazite, apatite, sulfide, ± ilmente, ± magnetite, ± topaz, ± columbite, and ± xenotime. Inter-intrusion and intra-intrusion variations in mineral chemistry are interpreted to reflect petrogenetic processes (e.g., assimilation and fractional crystallization) during granitoid evolution. Although magmatic equilibration among rock-forming minerals are disturbed by subsolidus hydrothermal processes, GMS rocks appear to have higher magmatic temperatures, variable levels of emplacement, a range of f_{O_2} (i.e., reduced intrusions $10^{-16.7}$~$10^{-13.4}$ and oxidized intrusions $10^{-14.0}$~$10^{-10.5}$ bars), and relatively low f_{HF}/f_{HCl} ratios ($10^{-3.0}$~$10^{-1.0}$) in exsolved fluids, compared to GS rocks. Reduced GMS intrusions bear higher gold potential and thus may be prospective targets for intrusion-related gold systems.

Electronic Supplementary Material Supplementary material is available for this article at http://dx.doi.org/10.1007/s00410-005-0018-7

Editorial responsibility: J. Hoefs

X.-M. Yang (✉) · D. R. Lentz
Department of Geology, University of New Brunswick, PO Box 4400, Fredericton, NB E3B 5A3, Canada
E-mail: xyang@inco.com
Tel.: +1-705-6828459
Fax: +1-705-6828243

X.-M. Yang
INCO Technical Service Ltd., Exploration, Highway 17 West, Copper Cliff, ON P0M 1N0, Canada

Introduction

The nature of ore fluids is an essential issue in the study of mineral deposits. Three approaches are commonly used to constrain the characteristics of ore fluids: stable isotopes, fluid inclusions, and mineral chemistry (e.g., halogen contents in biotite, amphibole, and apatite). Stable isotope and fluid inclusion studies are mostly employed to determine the source, physiochemical conditions, and evolution of ore fluids. However, it is noteworthy that mineral chemical equilibria can also be utilized to evaluate fluid evolution associated with magmatic rocks (Gunow et al. 1980; Munoz and Swenson 1981; Munoz 1984; Speer 1984, 1992; Keith and Shanks 1988; Keith et al. 1989, 1998; van Middlelaar and Keith 1990; Lentz 1992, 1994; Shaw and Penczak 1996; Piccoli et al. 1999; Coulson et al. 2001 and references therein); this is particularly important in evaluating the petrogenesis of intrusion-related gold systems (Müller and Groves 1993, 2000; McCoy et al. 1997; Coulson et al. 2001; Yang et al. 2002a). The principle of this method is to use internally consistent thermodynamic data, for those minerals containing hydroxyl and halogens (Zhu and Sverjensky 1991), to predict the fluoride and chloride activity of aqueous fluids from the measured F and Cl contents in the minerals. Coulson et al. (2001) used this method in their investigation of the fluid evolution of a gold-related granitic intrusion in the Tombstone Plutonic Suite, Yukon. However, this method is applicable only to

equilibrium mineral assemblages. Ternary-feldspar geothermometry (Fuhrman and Lindsley 1988) can test for equilibrium by assessing the extent of subsolidus recrystallization and (or) exchange processes.

Recent studies show a high potential for intrusion-related gold systems in southwestern New Brunswick, a part of the Canadian Appalachians (McLeod and McCutcheon 2000; Chi 2002; Lentz et al. 2002; Thorne et al. 2002; Davis et al. 2004; Yang et al. 2002a, b, 2003, 2004a, b), which is well known for W-Sn-Mo-Sb mineral resources associated with granitoids (McLeod 1990; Whalen 1993). Many gold occurrences and deposits in the area (e.g., Clarence Stream, Lake George, Poplar Mountain, McDougall Brook, Jimmy Hill, Kedron, Tower Hill; Fig. 1) share some similarities with intrusion-related gold systems elsewhere (McCoy et al. 1997; Thompson et al. 1999; Lang et al. 2000; Thompson and Newberry 2000; Baker 2002; Lang and Baker 2001; Fan et al. 2003; Bierlein et al. 2003; Groves et al. 2003; Doebrich et al. 2004). This has stimulated exploration efforts for intrusion-related gold deposits in this region. However, an essential question about intrusion-related gold systems is whether these intrusions supply mineralizing components. This contribution elaborates on detailed mineralogy and petrology of the two main groups of granitoids from the region, which yielded geothermobarometric constraints on their emplacement conditions, physiochemical conditions of crystallization and subsequent hydrothermal fluid evolution, and their implications on gold mineralization.

Geological setting

In southwestern New Brunswick, two major granitoid batholiths and associated satellite plutons are intruded into the Gander and Avalon zones of the Canadian Appalachian Orogen (Williams et al. 1999) (Fig. 1). The

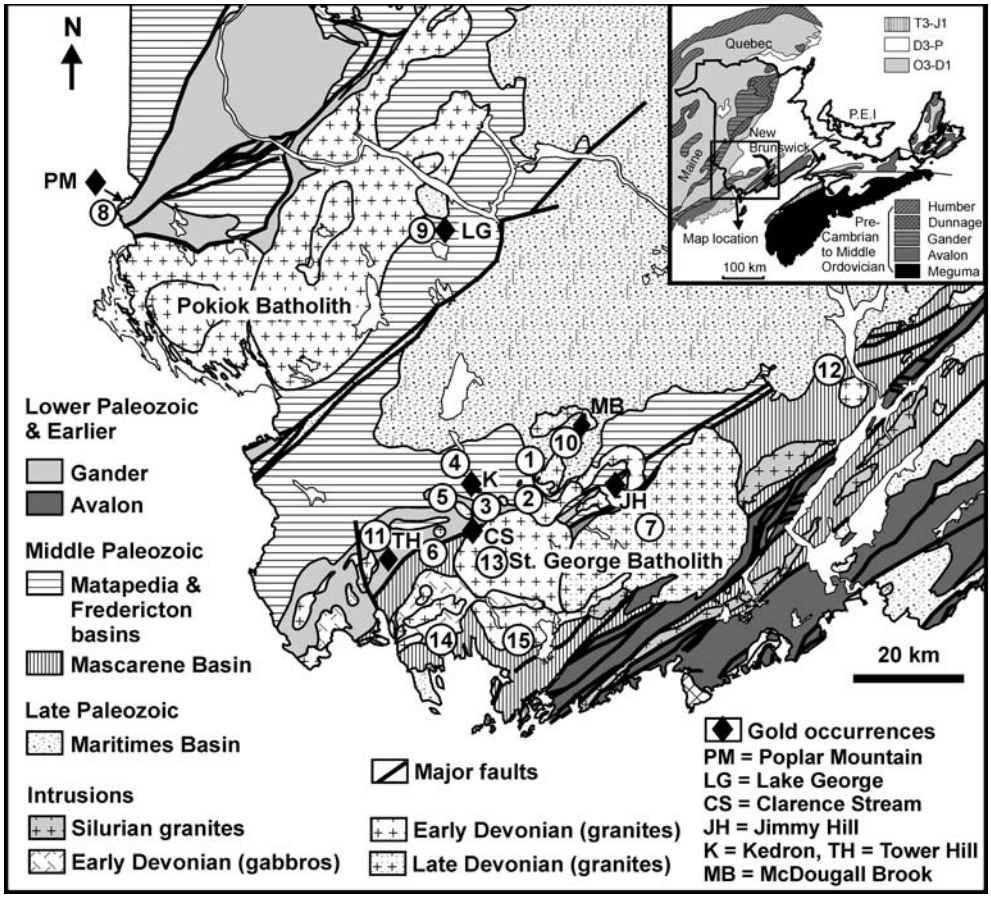

Fig. 1 Regional geological map of southwestern New Brunswick (modified from New Brunswick Department of Natural Resources and Energy 2000 and Chi 2002), showing the location of two series of granitoid intrusions, i.e., Late Devonian Granitic series (*GS*) granites: *1* Mount Pleasant Granite Suite (*MPG*), *2* True Hill Granite (*TRHG*), *3* Beech Hill Granite (*BHG*), *4* Kedron Granite (*KG*), *5* Pleasant Ridge Granite (*PRG*), and *6* Sorrel Ridge Granite (*SRG*) on the northwest margin of Sainte George Batholith (*SGB*), and *7* Mount Douglas Granites (*MDG*), the eastern part of the SGB; Late Silurian to Early Devonian Granodioritic to Monzogranitic series (*GMS*) granitoids: *8* Poplar Mountain Volcanic Suite (*PMVS*), *9* Lake George Granodiorite (*LG*), *10* McDougall Brook Granitoid Suite (*MBG*), *11* Tower Hill Granite (*THG*), *12* Evandale Granodiorite (*EG*), *13* Magaguadavic Granitoid Suite (*MGS*), *14* Bocabec Granitoid Suite (*BGS*), and *15* Utopia Granite (*UG*); MGS, BGS, and UG constitute a western part of the SGB. The location of gold deposits and (or) occurrences discussed in this study are also shown: *PM* Poplar Mountain, *LG* Lake George, *CS* Clarence Stream, *MB* McDougall Brook, *K* Kedron, *JH* Jimmy Hill, and *TH* Tower Hill

Pokiok Batholith intruded the Cambrian to Middle Ordovician strata of the Gander Zone and Late Silurian strata of the Fredericton Basin (Fyffe and Fricker 1987). Radiometric ages of this batholith are between 415 and 402 Ma (Whalen 1993; McLeod et al. 1994). The Saint George Batholith (Cherry 1976; McLeod 1990; Whalen 1993) intruded the Precambrian strata of the Caledonian Terrane, Ordovician strata of the St. Croix Terrane, and Late Silurian strata of the Mascarene Basin (Fyffe and Fricker 1987; Fyffe et al. 1999; Miller and Fyffe 2002). It is a composite batholith with isotopic ages between 423 and 360 Ma (McLeod 1990; Whalen 1993; McLeod et al. 1994; Davis et al. 2004).

On the basis of field relations, petrologic and petrochemical features as well as ages, two major groups of granitoid intrusions associated with gold mineralization in the region are recognized: (1) Late Devonian granitic series (GS), and (2) Late Silurian to Early Devonian granodioritic to monzogranitic series (GMS) rocks (Yang et al. 2004b). The GS intrusions include Mount Pleasant Granite Suite, True Hill Granite, Beech Hill Granite, Kedron Granite, Pleasant Ridge Granite, Sorrel Ridge Granite, and Mount Douglas Granites (i.e., labeled 1 to 7 in Fig. 1; Butt 1976; Lentz and McAllister 1990; McLeod 1990; Lentz and Gregoire 1995; Whalen et al. 1996), which collectively show high-level and highly evolved characteristics and are fractionated I-type granites; they intrude into Ordovician to Devonian sedimentary rocks (e.g., quartzite, slate, siltstone, and greywackes) along NE-trending fault zones (Fig. 1). These intrusions display a variety of textural phases ranging from equigranular, seriate to porphyritic, with variable accessory mineralogy. The emplacement of these felsic magmas might have taken place either post-orogenically or during the waning stage of the Acadian Orogeny, which are restricted to continental margin to within-plate environment (Fyffe and Fricker 1987; McLeod 1990; Whalen 1993; van Staal 1994; Fyffe et al. 1999; Yang et al. 2003, 2004b). All of the granites are subsolvus granites because of the presence of discrete plagioclase and K-feldspar crystals.

Granodioritic to monzogranitic series granitoids (labeled 8 to 15 in Fig. 1) include the western part of Saint George Batholith (i.e., Magaguadavic Granite Suite, Bocabec Granitoid Suite, Utopia Granite), Tower Hill Granite, McDougall Brook Granitoid Suite, Evandale Granodiorite, Lake George Granodiorite, and Poplar Mountain Volcanic Suite associated with the Pokiok Batholith (Butt 1976; Cherry 1976; McLeod 1990; Whalen 1993; McLeod et al. 1994; Chi 2002; Yang et al. 2002a, b, 2003, 2004b). Most GMS rocks are granodiorite, although a few are monzogranite, monzonite, quartz diorite, diorite, and gabbro (i.e., the Bocabec Granitoid Suite) (McLeod 1990; Whalen 1993; Thorne and Lentz 2001; Yang et al. 2002a, b). They intruded Cambrian to Upper Silurian greywacke, siltstone, shale, and mafic to felsic volcanoclastic rocks, which have been deformed and metamorphosed to greenschist grade during the Acadian Orogeny (Fyffe and Fricker 1987). They are typically less evolved in composition and show more variable emplacement levels; they are oxidized to reduced I-type granitoids. Petrologically, hornblende is typically present, and plagioclase is more abundant relative to K-feldspar in most GMS rocks.

Petrography

Granitic series rocks are characterized by the presence of high abundances of quartz, K-feldspar, and acidic plagioclase with variable minor and accessory minerals. They are mostly monzogranite, but some are syenogranite on the basis of the classification scheme by the IUGS sub-committee (Le Maitre et al. 2002). Fe-rich biotite and Li-bearing muscovite are present, but amphibole is absent. Primary topaz occurs in some of the intrusions (e.g., the Mount Pleasant Granite Suite, Pleasant Ridge Granite, Kedron Granite; Sinclair et al. 1988; Taylor 1992; Yang et al. 2003). They generally are similar to haplogranites and can be termed subsolvus granites as they contain two distinctive feldspars, and exhibit variable textural varieties (i.e., fine- to coarse-grained, equigranular, seriate, and porphyritic; Fig. 2a, b), reflecting highly evolved compositional characteristics and high-level of emplacement. Aplite, pegmatite, miarolitic cavities, comb quartz layers and quartz veins, unidirectional solidification textures, micrographic (Fig. 2c), and myrmekitic (Fig. 2d) textures (see Butt 1976; Lentz et al. 1988; Sinclair et al. 1988; McCutcheon et al. 2001; Yang et al. 2003) commonly occur and (or) are associated with GS intrusions, suggesting water saturation during crystallization (Kirkham and Sinclair 1988; Keith and Shanks 1988; Keith et al. 1989; Lentz and Fowler 1992; Candela and Piccoli 1995; Candela 1997). Interestingly, GS rocks are comparable to the evolved phases of the Mount Douglas Granite in the Saint George Batholith with respect to mineralogy, texture, and geochemistry, suggesting a possible genetic linkage (McLeod et al. 1988; Lentz and McAllister 1990; McLeod 1990; Lentz and Gregoire 1995; Yang et al. 2003, 2004b).

Granodioritic to monzogranitic series rocks are less evolved and have variable emplacement levels. Hybridization with country rocks commonly occurs at their marginal phases. The Tower Hill intrusion is characterized by the presence of muscovite and garnet that occur in the marginal phase, whereas the Bocabec Granitoid Suite comprises various rocks from gabbro to monzogranite. Highly fractionated phases occur in the Magaguadavic Granite Suite as well as the other intrusions. Mineralogically, the GMS rocks contain hornblende (Fig. 2e), variable contents of biotite (Fig. 2f–h), and more abundant plagioclase than K-feldspar. Therefore, they generally are subsolvus granites as well, except for mafic gabbro in the Bocabec Granitoid Suite. Primary magnetite is present in some of the GMS rocks (e.g., the Magaguadavic Granite Suite, Bocabec Granitoid Suite) (Cherry 1976; McLeod 1990; Thorne et al. 2002), but it is absent in the others that are dominated

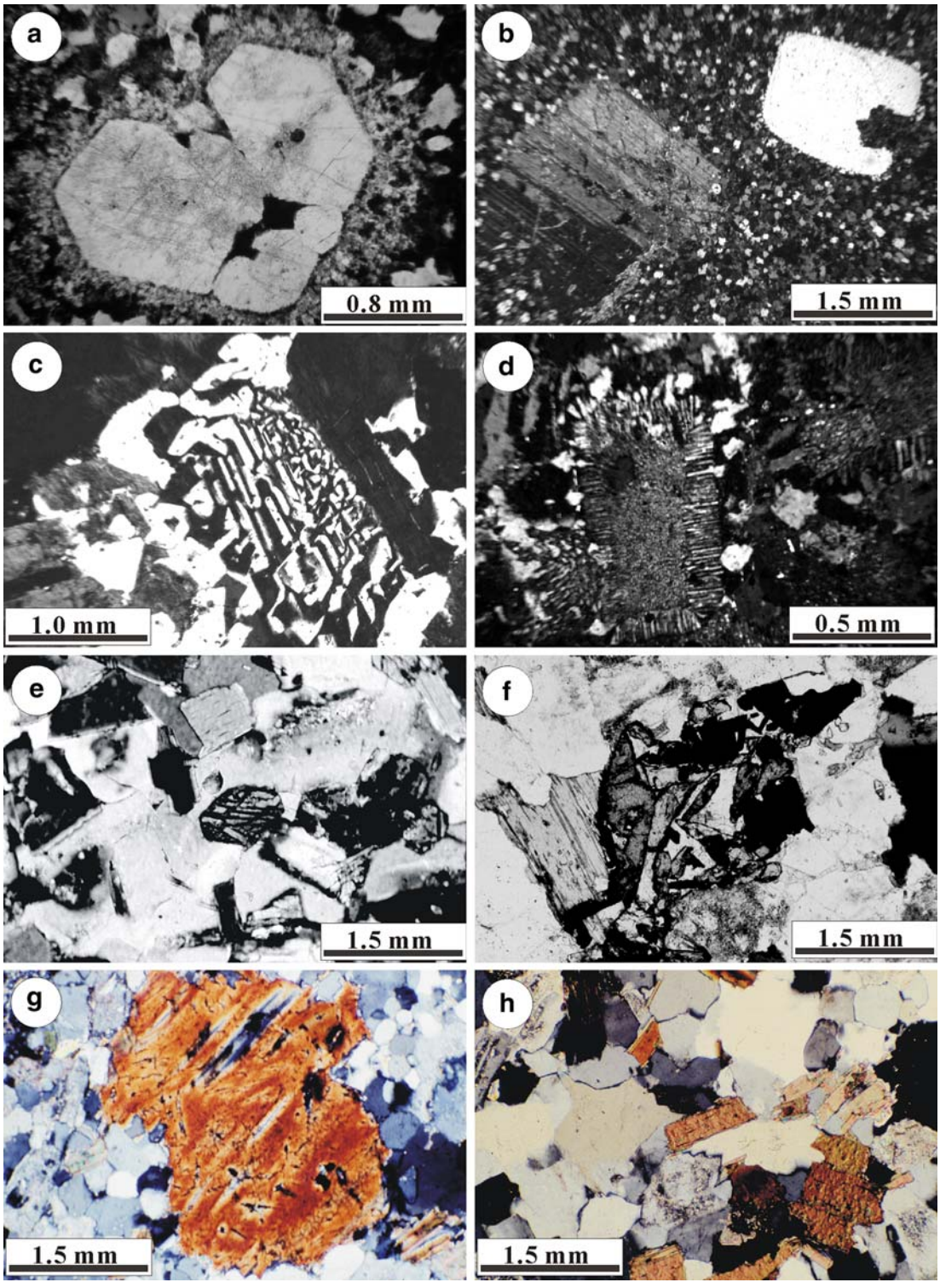

Fig. 2 Photomicrographs of some southwestern New Brunswick granitoids, illustrating the mineralogy and textures. **a** Partly resorbed euhedral quartz phenocryst (rich in secondary fluid inclusions) sitting in very fine-grained groundmass from the Mount Pleasant Granite, sample LNZ18-1843, plane-polarized light (PPL); **b** subhedral plagioclase and quartz (resorbed) phenocrysts in the Mount Pleasant Granite, sample PRL95-21962, PPL; **c** micrographic texture in the Mount Pleasant Granite, sample NMP89-1-1849, cross-polarized light (XPL); **d** myrmekitic texture (where the plagioclase is strongly altered to sericite, carbonate, and albite) in the Mount Pleasant Granite, sample NMP89-1-1849; **e** seriate to porphyritic texture, euhedral hornblende enclosed in plagioclase from the Lake George Granodiorite, sample LG81-19-1351, XPL; **f** biotite associated with euhedral titanite (*left side*) as well as altered relict biotite associated with anhedral titanite, magnetite, and chlorite, and calcite; **g** subhedral fox-red biotite phenocryst in fine-grained felsic groundmass consisting of quartz, orthoclase, plagioclase, and opaques, sample LG81-12-1567, XPL; **h** suhedral pinkish to greenish biotite in granite from the Bocabec Granitoid Suite, sample 85-202, XPL

by ilmenite (e.g., the Lake George Granodiorite) (Seal et al. 1987; Yang et al. 2002a, b). Aplite and pegmatite dikes, as well as late sulfide-bearing quartz veins, are commonly associated with these intrusions.

Petrochemical characteristics

Petrochemical difference between GMS and GS rocks is evident (Yang et al. 2004b). GMS rocks are calcalkaline, metaluminous to weakly peraluminous, characterized by relatively low silica (< 70 wt%), high CaO (< 4.39 wt%), low contents of incompatible elements, moderate to high $(La/Yb)_N$ (3.5–35.8) and Zr/Hf (20.1–48.9) ratios, and a pronounced negative Nb anomaly and small Eu, Ti, Sr, and Ba anomalies. In contrast, the GS rocks, although mostly calcalkaline, metaluminous to peraluminous, contain high silica (> 72 wt%), incompatible elements and high field strength elements, and low CaO (< 1.88 wt%), TiO_2 (< 0.22 wt%), with low $(La/Yb)_N$ (< 7.3) and Zr/Hf (12.8–43.0) ratios, without a negative (or very small) Nb anomaly, but more pronounced negative Eu, Ti, Sr, and Ba anomalies.

Analytical procedures

Electron probe microanalysis (EPMA) of mineral compositions was conducted in wavelength-dispersion mode on a JXA JEOL-733 Superprobe at the University of New Brunswick, with 15 kV accelerating voltage, 10 nA beam current, and a maximum 40-s counting interval. The beam size was set to be 5 μm. A combination of various mineral and metal standards were used with ZAF matrix corrections by means of CITZAF version 3.03 (J.T. Armstrong, 1997, shareware; Division of Earth and Planetary Sciences, the California Institute of Technology). The analytical limits are on the order of 0.05 wt%. In each sample, several grains of each mineral were analyzed based on textural relation and grain positions. An average of the analytical results was taken to represent the typical composition of that mineral in each sample, together with standard deviation. Formula calculations of amphibole are based on 23 atoms of oxygen, and their ferric/ferrous ratios are calculated using 13-cation normalization and charge balance. Formula calculations of biotite are based on 22 atoms of oxygen, their H_2O contents were calculated by stoichiometry, and ferric/ferrous ratios are computed by charge balance. Albite, orthoclase, and anorthite mole fractions in feldspars are calculated.

Characteristics of mineral chemistry

Table. 1, 2, 3, and 4 tabulate the representative EPMA analyses of major rock-forming and accessory minerals in GS and GMS granitoids (Fig. 1). Detailed analytic data of the rock-forming minerals are deposited in a data bank as eTables 1, 2, and 3, which is also available from the authors upon request. The chemical features of these minerals are summarized as follows.

Rock forming minerals

Micas

Micas in the granitoid samples usually have tiny mineral inclusions, such as apatite, zircon, monazite, titanite, magnetite, ilmenite, xenotime, and sulfide minerals (e.g., pyrrhotite, pyrite). Interestingly, the color of biotite is variable in GMS intrusions from fox-red (Fig. 2g) to brown (e.g., the reduced I-type Lake George Granodiorite; see Yang et al. 2002b, 2004a) through dark brown to greenish (Fig. 2h) (e.g., the oxidized I-type Magaguadavic Granite Suite, Bocabec Granitoid Suite), reflecting differences in their redox conditions (cf. Lalonde and Bernard 1993). Biotite is usually light brown to fox-red, if present in GS rocks, indicative of its relatively reduced nature. According to the classification scheme of International Mineralogical Association (IMA) (Rieder et al. 1998), trioctahetral biotite in the studied granitoids is located within the series annite $[KFe^{2+}{}_3AlSi_3O_{10}(OH)_2]$, siderophyllite $[KFe^{2+}{}_2Al_2Si_2O_{10}(OH)_2]$, phlogopite $[KMg_3AlSi_3O_{10}(OH)_2]$, and eastonite $[KMg_2AlAl_2Si_2O_{10}(OH)_2]$ (Fig. 3). It is common that secondary chlorite and (or) fine-grained muscovite replaced biotite minerals along their cleavage planes and margins.

Chemical composition of micas in GS rocks varies systematically from Fe-rich biotite in the Mount Douglas, True Hill (Lentz et al. 1988), Beech Hill, Sorrel Ridge, and Mount Pleasant granites (Table 1), through Li-mica (i.e., zinnwaldite) in Kedron and Pleasant Ridge granites (Table 1) (Taylor 1992). Although intra-intrusion variations in the Mg/(Mg + Fe) ratios (atomic) of biotite (Table 1 and eTable 1) are present, the ratios decrease from the Mount Douglas (0.44 ± 0.02–0.09 ± 0.01) through Beech Hill (0.43 ± 0.06), to Sorrel Ridge (0.26 ± 0.01–0.18 ± 0.01) and Mount Pleasant (0.01 ± 0.02). In addition, the biotite is characterized by appreciable F contents, up to 2.18 ± 0.13 wt% (e.g., Mount Douglas; Table 1). ΣAl of biotite is < 3.0 apfu (atoms per formula unit), except for the biotite in the Mount Pleasant Granite Suite, which is close to the end member of siderophyllite (Fig. 3). F contents also decrease from the Mount Douglas to Sorrel Ridge Granite (0.39 ± 0.15 wt%), but F is high in biotite (4.39 ± 0.75 wt%) in the Mount Pleasant Granite owing to extreme fractionation (Yang et al. 2003). Li-mica occurs in highly evolved intrusions, such as the Pleasant Ridge and Kedron Granites, which are characterized by high F contents (up to 7.73 ± 0.17 wt%), Li_2O (2.84 wt%; Taylor, 1992), and very low Mg/(Mg + Fe) ratios ($< 0.04 \pm 0.01$ wt%; Table 1 and eTable 1). Muscovite is present in the Kedron and Mount Pleasant granites as well, but this F-rich muscovite (up to

Table 1 Representative chemical composition (wt%) and structural formulae of micas in granitoids from southwestern New Brunswick

Intrusions	Mount Pleasant		Beech Hill		Pleasant Ridge		Sorrel Ridge		Mount Dougals		Lake George		Tower Hill		Evandale		Magagua-davic		Bocabec		Utopia	
Samples	AM96-3-1233		BH01-111		C82-5-75		C80-10-353		85-197		LG81-12-1567		C80-5-254		SEV01-125		85-195		85-178		85-189	
Minerals	Biotie		Biotite		Li-Mica		Biotite		Biotite		Biotite		Biotite		Biotite		Biotite		Biotite		Biotite	
No. of grains	2		1		2		1		2		4		3		2		4		2		2	
n	4		2		2		2		4		7		6		4		12		4		4	
	Av.	1σ	Av.	1 σ	Av.	1 σ	Av.	1 σ	Av.	1 σ	Av.	1 σ	Av.	1 σ	Av.	1 σ	Av.	1 σ	Av.	1 σ	Av.	1 σ
SiO_2	42.0	1.9	37.6	0.1	43.1	1.3	35.8	0.6	36.5	0.1	35.9	0.8	35.3	1.5	36.8	0.6	35.4	1.4	35.6	0.4	37.5	0.6
TiO_2	0.26	0.07	3.01	0.04	0.26	0.03	3.11	0.37	3.07	0.93	4.00	0.24	2.86	0.52	3.86	0.95	3.20	0.64	4.88	0.21	3.26	0.33
Al_2O_3	23.97	0.63	15.98	0.36	22.55	1.10	14.48	0.44	13.41	0.28	15.69	0.87	19.42	0.31	13.91	0.52	13.57	0.62	14.14	0.14	14.62	0.63
Cr_2O_3	0.01	0.01	0.03	0.05	0.00	0.00	0.01	0.01	0.00	0.00	0.02	0.02	0.03	0.06	0.04	0.03	0.01	0.02	0.03	0.02	0.00	0.01
Fe_2O_3	16.88	2.92	10.81	0.93	0.00	0.00	11.96	0.55	15.16	0.33	2.96	2.04	4.29	1.37	0.00	0.00	6.23	1.54	0.57	0.11	18.06	1.17
FeO	0.12	0.78	15.78	0.94	14.89	0.15	18.79	1.33	7.58	0.87	18.92	2.82	17.57	0.62	20.95	3.74	19.38	6.30	21.21	0.24	6.56	1.43
MnO	0.89	0.20	0.46	0.02	1.12	0.00	0.71	0.10	0.70	0.18	0.38	0.07	0.49	0.16	0.38	0.15	0.54	0.20	0.14	0.03	0.77	0.12
MgO	0.10	0.11	4.87	0.17	0.06	0.05	3.70	0.13	10.18	0.48	9.59	0.50	4.35	0.14	11.47	2.67	7.53	5.11	9.80	0.18	6.19	0.56
CaO	0.11	0.16	0.04	0.01	0.09	0.11	0.21	0.19	0.09	0.10	0.06	0.04	0.01	0.01	0.14	0.18	0.73	1.73	0.03	0.05	0.00	0.00
Na_2O	0.30	0.10	0.06	0.02	0.23	0.05	0.08	0.01	0.05	0.01	0.11	0.06	0.03	0.02	0.10	0.02	0.06	0.02	0.09	0.01	0.08	0.04
K_2O	8.70	0.59	8.91	0.08	9.24	0.28	7.52	1.05	8.65	0.76	8.07	0.70	8.77	0.68	8.94	0.77	7.94	0.99	8.45	0.44	9.11	0.18
H_2O	2.12	0.35	3.39	0.06	0.88	0.09	3.22	0.09	2.89	0.09	3.80	0.06	3.64	0.09	4.14	0.36	3.52	0.18	3.85	0.03	2.59	0.18
Cl	0.09	0.03	0.32	0.02	0.01	0.01	0.40	0.02	0.15	0.03	0.06	0.01	0.02	0.02	0.00	0.00	0.20	0.19	0.09	0.02	0.14	0.17
F	4.39	0.75	1.03	0.15	7.20	0.22	1.09	0.09	2.18	0.13	0.24	0.20	0.39	0.15	0.00	0.00	0.49	0.09	0.00	0.00	2.90	0.49
-O = Cl	0.02	0.01	0.07	0.00	0.00	0.00	0.09	0.00	0.03	0.01	0.01	0.00	0.00	0.01	0.00	0.00	0.05	0.04	0.02	0.00	0.03	0.04
-O = F	1.85	0.32	0.43	0.06	3.03	0.09	0.46	0.04	0.92	0.05	0.10	0.08	0.16	0.06	0.00	0.00	0.21	0.04	0.00	0.00	1.22	0.20
Total	100.0		102.3		99.7		101.0		100.6		99.8	1.2	97.1		100.7		98.8		98.9		101.8	
^{IV}Si	5.967	0.231	5.680	0.029	6.022	0.164	5.591	0.023	5.524	0.056	5.477	0.066	5.516	0.194	5.358	0.492	5.579	0.056	5.511	0.035	5.623	0.046
^{IV}Al	2.033	0.231	2.320	0.029	1.978	0.164	2.409	0.023	2.476	0.056	2.523	0.066	2.484	0.194	2.642	0.492	2.421	0.056	2.489	0.035	2.377	0.046
T_{site}	8.000	0.000	8.000	0.000	8.000	0.000	8.000	0.000	8.000	0.000	8.000	0.000	8.000	0.000	8.000	0.000	8.000	0.000	8.000	0.000	8.000	0.000
^{VI}Al	1.978	0.316	0.526	0.030	1.732	0.028	0.257	0.088	−0.083	0.111	0.294	0.099	1.096	0.174	−0.255	0.694	0.100	0.085	0.092	0.009	0.204	0.145
Ti	0.028	0.007	0.343	0.005	0.027	0.003	0.365	0.040	0.348	0.103	0.459	0.033	0.337	0.062	0.419	0.087	0.382	0.085	0.568	0.023	0.367	0.040
Cr	0.001	0.001	0.004	0.006	0.000	0.000	0.001	0.001	0.000	0.000	0.002	0.002	0.003	0.008	0.604	1.200	0.001	0.002	0.004	0.002	0.000	0.001
Fe^{3+}	1.991	0.332	0.574	0.068	0.000	0.000	0.645	0.054	1.082	0.073	0.131	0.096	0.197	0.071	0.000	0.000	0.301	0.081	0.023	0.005	1.407	0.192
Fe^{2+}	0.029	0.286	2.788	0.076	1.738	0.192	3.371	0.110	1.797	0.122	2.660	0.238	2.663	0.125	2.541	0.441	3.107	1.039	2.798	0.039	1.678	0.263
Mn	0.107	0.025	0.059	0.003	0.132	0.000	0.094	0.014	0.090	0.023	0.049	0.009	0.065	0.021	0.048	0.021	0.073	0.029	0.018	0.004	0.097	0.016
Mg	0.022	0.022	1.098	0.040	0.013	0.010	0.861	0.041	2.298	0.123	2.179	0.092	1.014	0.030	2.508	0.690	1.736	1.144	2.262	0.049	1.381	0.119
O_{site}	4.157	0.130	5.391	0.031	3.642	0.142	5.593	0.047	5.532	0.044	5.773	0.135	5.375	0.052	5.864	0.083	5.700	0.230	5.765	0.061	5.134	0.066
Ca	0.017	0.024	0.006	0.001	0.013	0.016	0.035	0.032	0.015	0.017	0.009	0.007	0.002	0.002	0.021	0.029	0.120	0.286	0.004	0.009	0.000	0.000
Na	0.082	0.027	0.019	0.006	0.061	0.013	0.025	0.004	0.015	0.003	0.031	0.018	0.009	0.005	0.027	0.006	0.017	0.007	0.026	0.004	0.024	0.011
K	1.577	0.110	1.718	0.013	1.644	0.045	1.496	0.193	1.669	0.135	1.570	0.142	1.751	0.148	1.658	0.175	1.599	0.211	1.669	0.075	1.739	0.026
A_{site}	1.676	0.106	1.743	0.009	1.718	0.048	1.556	0.165	1.699	0.119	1.618	0.147	1.762	0.146	1.706	0.157	1.736	0.317	1.699	0.069	1.764	0.024
OH^-	2.009	0.332	3.426	0.068	0.823	0.090	3.355	0.054	2.918	0.073	3.869	0.096	3.803	0.071	4.000	0.000	3.699	0.081	3.977	0.005	2.593	0.192
Cl	0.022	0.007	0.082	0.004	0.002	0.002	0.105	0.006	0.037	0.009	0.015	0.003	0.004	0.006	0.000	0.000	0.055	0.052	0.023	0.005	0.036	0.042
F	1.969	0.337	0.492	0.072	3.176	0.088	0.540	0.049	1.045	0.068	0.116	0.095	0.193	0.075	0.000	0.000	0.246	0.047	0.000	0.000	1.371	0.224
Mg/(Mg + Fe)	0.01	0.02	0.25	0.01	0.01	0.01	0.18	0.01	0.44	0.02	0.44	0.01	0.26	0.01	0.49	0.11	0.34	0.22	0.44	0.00	0.31	0.02

Formula calculations are based on 22 oxygens, H_2O contents were calculated by stoichiometry, and ferric/ferrous ratios were computed in terms of charge balance. Complete data see eTable 1

1.95 ± 0.23 wt%) may be attributed to alteration of Li-mica.

Mica minerals in GMS rocks are dominated by biotite. Generally, biotite has high Mg/(Mg + Fe) ratios, although both inter- and intra-intrusion variations are evident (Table 1 and eTable 1; Yang et al. 2002b). ΣAl of the biotite is < 3.0 apfu, except for those in the Tower Hill Granite that also show relatively low high Mg/(Mg + Fe) ratios (Table 1). The F contents of biotite are variable in different intrusions. Biotite in the Utopia Granite contains the highest F contents of 2.90 ± 0.49 wt%. Primary muscovite only occurs in the marginal phase of the Tower Hill Granite, together with almandine-spessartine series garnet. The muscovite is poor in F contents, but has high Mg/(Mg + Fe) ratios relative to muscovite in GS rocks (Table 1); biotite is rich in Al and Fe as well (Fig. 3), suggesting that a significant amount of supracrustal materials are required for the formation of the Tower Hill Granite through assimilation and crystallization processes (Yang et al. 2004b).

As shown in Fig. 3, the Fe/(Fe + Mg) ratios of biotite in GMS rocks decrease with increasing Σ Al (e.g., the Magaguadavic Granite Suite, Bocabec Granitoid Suite), but the Fe/(Fe + Mg) ratios increase with increasing Σ Al for GS rocks (e.g., the Mount Douglas Granite). As mentioned above the Tower Hill Granite is an exception for GMS rocks, which exhibits Fe/(Fe + Mg) ratios increase with elevating Σ Al values too (Fig. 3).

Table 2 Representative chemical composition (wt%) and structural formulae of hornblende in granitoids from southwestern New Brunswick

Intrusions	Lake George		Evandale		Magaguadavic				Bocabec	
Samples	LG80-36-1647		SEV-01-125		85-195		85-196		85-178	
No. of Grains	1		4		4		4		2	
n	2		7		11		9		4	
	Av.	1 σ	Av.	1 σ	Av.	1 σ	Av.	1 σ	Av.	1 σ
SiO_2	44.2	0.7	50.1	1.8	46.1	1.8	45.1	3.1	49.9	2.6
TiO_2	1.52	0.14	0.99	0.31	1.12	0.18	0.88	0.48	1.26	0.27
Al_2O_3	9.61	0.45	5.29	1.39	5.95	0.98	5.36	1.08	7.84	3.75
Cr_2O_3	0.02	0.01	0.03	0.02	0.01	0.01	0.02	0.01	0.01	0.01
Fe_2O_3	2.66	0.01	0.00	0.00	1.45	0.64	0.90	0.69	0.57	0.11
FeO	17.34	0.65	14.93	0.98	13.98	0.80	16.38	2.20	15.46	2.87
MnO	0.90	0.09	0.53	0.05	0.77	0.14	0.90	0.05	0.31	0.08
MgO	8.96	0.23	14.45	1.11	12.59	0.49	11.60	0.98	10.41	2.70
CaO	11.21	0.03	11.83	0.16	11.59	0.21	11.46	0.31	9.98	1.65
Na_2O	1.44	0.01	1.23	0.23	0.94	0.21	0.83	0.18	1.77	1.66
K_2O	0.98	0.08	0.49	0.15	0.47	0.12	0.43	0.12	0.35	0.06
Cl	0.04	0.01	0.00	0.00	0.07	0.02	0.03	0.05	0.09	0.02
F	0.00	0.00	0.00	0.00	0.09	0.05	0.06	0.05	0.00	0.00
-O = F,Cl	0.01	0.00	0.00	0.00	0.05	0.03	0.03	0.03	0.02	0.00
Total	98.8		99.8		95.2		93.9		97.9	
Si	6.638	0.097	7.211	0.207	7.043	0.154	7.050	0.227	7.284	0.154
^{IV}Al	1.362	0.097	0.789	0.207	0.957	0.154	0.950	0.227	0.716	0.154
T site	8.000		8.000		8.000		8.000		8.000	
^{VI}Al	0.341	0.014	0.111	0.052	0.114	0.067	0.043	0.099	0.621	0.731
Ti	0.172	0.016	0.107	0.034	0.128	0.020	0.104	0.059	0.139	0.033
Fe^{3+}	0.163	0.001	0.000	0.000	0.060	0.027	0.037	0.029	0.022	0.004
Cr	0.002	0.000	0.003	0.003	0.001	0.001	0.002	0.001	0.002	0.002
Fe^{2+}	2.205	0.057	1.800	0.131	1.912	0.095	2.229	0.283	1.947	0.392
Mn	0.110	0.014	0.065	0.006	0.100	0.020	0.119	0.008	0.038	0.010
Mg	2.005	0.050	2.914	0.203	2.685	0.066	2.465	0.176	2.232	0.321
C site	5.000		5.000		5.000		5.000		5.000	
Mg	0.000	0.000	0.188	0.020	0.181	0.033	0.238	0.147	0.051	0.326
Fe^{2+}	0.147	0.029	0.000	0.000	0.000	0.000	0.000	0.000	0.000	0.000
Mn	0.000	0.000	0.000	0.000	0.000	0.000	0.000	0.000	0.000	0.000
Ca	1.806	0.001	1.812	0.020	1.819	0.033	1.762	0.147	1.949	0.326
Na	0.048	0.028	0.000	0.000	0.000	0.000	0.000	0.000	0.000	0.000
B site	2.000		2.000		2.000		2.000		2.000	
Ca	0.000	0.000	0.013	0.030	0.079	0.067	0.162	0.129	0.000	0.622
Na	0.386	0.052	0.344	0.067	0.277	0.059	0.251	0.054	0.491	0.441
K	0.189	0.017	0.091	0.029	0.091	0.024	0.085	0.023	0.065	0.013
Asite	0.575		0.448		0.368		0.336		0.556	
Mg/(Fe + Mg)	0.44	0.36	0.63	0.63	0.59	0.45	0.54	0.51	0.54	0.62

Formula calculations are based on 23 oxygen, and ferric/ferrous ratios are calculated using 13-cations normalization and charge balance (Leake et al. 1997). More data see eTable 2

Amphibole

Amphibole group minerals occur only in GMS intrusions and contain abundant mineral inclusions (e.g., plagioclase, titanite, apatite, zircon, magnetite, and pyrrhotite). They are commonly poor in F and Cl contents (Table 2 and eTable 2), and are calcic hornblende (edenite to ferro-paragasite; Fig. 4) according to the classification of Leake et al. (1997). Generally, hornblende has Ca in the site of M4 >1.0, with NaTable 2 and eTable 2; Fig. 4). It has moderate Al_2O_3 (<10 wt%) and TiO_2 (<2 wt%) contents (Table 2 and eTable 2). The Mg/(Mg + Fe) ratios (atomic) of hornblende are fairly consistent in different intrusions (i.e., Evandale, Magaguadavic, Bocabec), ranging from 0.54 to 0.63, which is apparently higher than those of hornblende (0.46 ± 0.07) from the Lake George Granodiorite (Table 2 eTable 2; Yang et al. 2002b). However, the Al_2O_3 contents of hornblende (Table 2) are relatively low, which may be ascribed to their crystallization at lower pressures based on Al-in-amphibole geobarometry (cf. Hammarstrom and Zen 1986).

Plagioclase

The presence of discrete plagioclase in both GS and GMS rocks is noted with typical albite twinning,

Table 3 Representative chemical composition (wt%) of feldspar in granitoids from southwestern New Brunswick and end-member mole ratios (X_{Ab}, X_{Or}, and X_{An})

Intrusions	Mount Pleasant				Beech hill				Kedron				Pleasant Ridge				Sorrel Ridge			
Sample	AM96-3-1233		AM96-3-1233		BH01-111		BH01-111		BR84-4-87		BR84-4-87		C82-4-14		C82-4-14		C81-9-258		C81-9-258	
Mineral	K-feldspar		Plagioclase		K-feldspar		Plagioclase		K-feldspar		Plagioclase		K-feldspar		Plagioclase		K-feldspar		Plagioclase	
No. of Grains	2		3		2		1		2		2		2		2		6		4	
n	5		5		3		3		6		6		6		6		11		11	
	Av.	1 σ	Av.	1 σ	Av.	1 σ	Av.	1 σ	Av.	1 σ	Av.	1 σ	Av.	1 σ	Av.	1 σ	Av.	1 σ	Av.	1 σ
SiO_2	65.8	0.2	66.6	0.4	65.3	0.7	66.4	1.0	64.1	0.7	67.0	0.6	65.8	1.8	66.0	0.4	64.4	1.2	65.6	1.7
TiO_2	0.01	0.02	0.00	0.01	0.00	0.00	0.00	0.00	0.01	0.01	0.01	0.01	0.03	0.06	0.00	0.00	0.01	0.03	0.00	0.01
Al_2O_3	19.37	0.14	21.39	0.37	19.66	0.29	21.48	0.57	19.67	0.09	20.89	0.22	19.41	0.87	21.20	0.15	18.89	0.60	20.83	0.61
Cr_2O_3	0.00	0.01	0.01	0.01	0.00	0.00	0.00	0.00	0.00	0.01	0.02	0.02	0.00	0.01	0.05	0.09	0.01	0.02	0.04	0.09
Fe_2O_3	0.06	0.02	0.19	0.12	0.05	0.05	0.23	0.04	0.00	0.00	0.02	0.02	0.00	0.01	0.02	0.04	0.05	0.06	0.03	0.04
MnO	0.01	0.01	0.02	0.02	0.01	0.01	0.01	0.02	0.01	0.01	0.01	0.01	0.00	0.00	0.03	0.06	0.00	0.01	0.04	0.08
MgO	0.00	0.00	0.01	0.02	0.00	0.00	0.00	0.00	0.00	0.00	0.00	0.00	0.00	0.00	0.00	0.00	0.00	0.00	0.00	0.01
CaO	0.01	0.02	0.23	0.20	0.01	0.01	0.92	0.24	0.01	0.01	0.05	0.03	0.07	0.16	0.20	0.13	0.09	0.15	0.35	0.28
Na_2O	0.16	0.04	12.25	0.25	0.44	0.41	11.90	0.28	0.18	0.01	12.88	0.18	0.29	0.20	13.01	0.15	0.83	0.80	12.38	0.28
K_2O	16.12	0.08	0.25	0.07	15.71	0.39	0.24	0.04	16.02	0.14	0.12	0.03	15.57	1.10	0.13	0.07	15.32	1.09	0.15	0.11
Total	101.6		100.9		101.2		101.2		100.0		101.0		101.2		100.6		99.6		99.5	
X_{Ab}	0.015	0.003	0.977	0.006	0.040	0.037	0.947	0.013	0.017	0.001	0.992	0.002	0.027	0.018	0.985	0.004	0.075	0.071	0.977	0.015
X_{Or}	0.984	0.003	0.013	0.004	0.959	0.036	0.013	0.002	0.983	0.001	0.006	0.002	0.969	0.017	0.007	0.003	0.920	0.071	0.008	0.006
X_{An}	0.001	0.001	0.010	0.009	0.001	0.001	0.040	0.011	0.001	0.000	0.002	0.001	0.004	0.010	0.008	0.005	0.004	0.008	0.015	0.012

Intrusions	Mount Douglas				Lake George				Tower Hill				Magaguadavic				Bocabec			
Sample	85-197		85-197		LG81-12-1567		LG81-12-1567		C80-2-580		C80-2-580		85-195		85-195		85-176		85-176	
Mineral	K-feldspar		Plagioclase		Plagioclase		K-feldspar		K-feldspar		Plagioclase		K-feldspar		Plagioclase		K-feldspar		Plagioclase	
No. of Grains	2		1		3 phenocrysts		2 phenocrysts		3		3		5		5		2		2	
n	5		2		9		4		6		6		12		13		4		4	
	Av.	1 σ	Av.	1 σ	Av.	1 σ	Av.	1 σ	Av.	1 σ	Av.	1 σ	Av.	1 σ	Av.	1 σ	Av.	1 σ	Av.	1 σ
SiO_2	64.3	0.7	59.4	0.5	59.7	3.2	63.8	1.0	62.9	1.9	66.1	0.3	64.0	1.1	61.7	2.3	65.0	0.3	64.0	1.0
TiO_2	0.03	0.03	0.02	0.00	0.01	0.03	0.03	0.03	0.05	0.06	0.02	0.02	0.06	0.11	0.01	0.02	0.00	0.00	0.00	0.00
Al_2O_3	20.02	0.08	24.91	0.37	24.75	2.30	18.51	0.07	18.80	0.22	20.30	0.30	19.76	0.29	23.89	0.79	19.68	0.11	23.00	0.71
Cr_2O_3	0.08	0.17	0.30	0.41	0.00	0.01	0.01	0.01	0.00	0.00	0.03	0.07	0.14	0.32	0.02	0.06	0.00	0.00	0.00	0.01
Fe_2O_3	0.07	0.04	0.23	0.01	0.15	0.07	0.07	0.06	0.01	0.02	0.04	0.06	0.12	0.07	0.15	0.07	0.07	0.03	0.12	0.04
MnO	0.10	0.21	0.08	0.10	0.01	0.01	0.02	0.02	0.02	0.03	0.10	0.24	0.00	0.01	0.01	0.02	0.01	0.01	0.01	0.01
MgO	0.01	0.01	0.00	0.00	0.04	0.05	0.01	0.01	0.00	0.00	0.01	0.02	0.01	0.02	0.01	0.01	0.00	0.00	0.00	0.00
CaO	0.06	0.02	4.73	0.21	5.17	1.27	0.06	0.04	0.01	0.01	0.79	0.21	0.07	0.06	3.47	1.19	0.04	0.03	2.74	0.92
Na_2O	0.70	0.35	8.86	0.01	8.03	0.91	0.78	0.22	0.98	0.82	12.22	0.20	1.61	0.94	9.33	0.90	0.98	0.13	10.04	0.78
K_2O	15.52	0.47	0.80	0.02	0.50	0.17	14.87	0.34	15.65	0.67	0.08	0.05	13.78	1.34	0.47	0.38	14.81	0.17	0.58	0.29
Total	100.9		99.3		98.4		98.1		98.4		99.7		99.5		99.1		100.6		100.5	
X_{Ab}	0.064	0.032	0.738	0.007	0.715	0.066	0.073	0.020	0.085	0.066	0.961	0.009	0.150	0.086	0.807	0.056	0.091	0.012	0.840	0.050
X_{Or}	0.933	0.031	0.044	0.001	0.029	0.010	0.924	0.022	0.915	0.066	0.004	0.003	0.847	0.086	0.028	0.025	0.907	0.013	0.032	0.016
X_{An}	0.003	0.001	0.218	0.008	0.255	0.065	0.003	0.002	0.000	0.000	0.034	0.009	0.003	0.003	0.165	0.055	0.002	0.001	0.128	0.044

Complete data see eTable 3

although they have distinct chemical compositions (Table 3 and eTable 3). In GS rocks, plagioclase ranges from albite to oligoclase (An = 1–22) generally, lacking crystal-chemical zoning. Plagioclase from highly differentiated intrusions, such as Mount Pleasant, Beech Hill, Sorrel Ridge, and Pleasant Ridge, is exclusively albite (An < 7) and is also low in Or components (< 2), although the plagioclase from a related aplite dyke contains high Or end-member (50) (Table 3). Taylor (1992) analyzed plagioclase in the Pleasant Ridge Granite and obtained a similar result (An < 3). It is worthy of note that plagioclase composition systematically changes from the Mount Douglas (An = 14–22), through Beech Hill (4), Sorrel Ridge (1–6), Kedron (~2), Mount Pleasant (0.8–1), and Pleasant Ridge Granites (0.5–1) (Table 3 and eTable 3), consistent with the degree of

Table 4 Selective results (wt%) of accessory minerals in granitoids from southwestern New Brunswick

Intrusions	Lake George				Tower Hill		Magaguadavic			
Sample	LG83-2-1995		LG80-36-1647		C80-5-279		85-186		85-195	85-197
Mineral	Ilmenite	Titanite	Ilmenite	Titanite	Garnet		Magnetite		Magnetite	Magnetite
No. of Grains	1	1	1		3		2		1	1
n	1	1	1		9		2		1	1
					Av.	1 σ	Av.	1 σ	(core)	(core)
SiO_2	0.0	30.0	0.1	30.1	35.7	0.1	0.0	0.0	0.0	0.1
TiO_2	49.70	36.53	47.04	35.76	0.05	0.02	0.13	0.13	0.05	0.10
Al_2O_3	0.00	1.55	0.03	1.5	20.47	0.09	0.03	0.02	0.02	0.09
Cr_2O_3	0.02	0.00	0.00	0	0.00	0.00	0.04	0.06	0.14	0.01
FeO	48.31	1.60	40.93	1.51	29.56	0.18	95.70	1.30	95.93	95.59
MnO	1.68	0.19	4.28	0.15	13.15	0.17	0.13	0.01	0.05	0.04
MgO	0.01	0.01	0.03	0	0.40	0.02	0.00	0.00	0.00	0.00
CaO	0.01	27.53	0.39	26.6	0.50	0.08	0.14	0.19	0.57	0.00
Na_2O	0.01	0.01	0.01	0.01	0.01	0.01	0.02	0.02	0.00	0.02
K_2O	0.00	0.00	0.00	0	0.00	0.00	0.00	0.00	0.00	0.00
Total	99.7	97.4	92.8	95.6	99.9		96.2		96.8	96.0

Intrusions	Magaguadavic								Bocabec	
Sample	85-186		85-195		85-196		85-197		85-178	
Mineral	Titanite		Titanite		Titanite		Titanite		Magnetite	
No. of Grains	1		3		1		3		2	
n	3		3		2		6		2	
	Av.	1 σ	Av.	1 σ	Av.	1 σ	Av.	1 σ	Av.	1 σ
SiO_2	27.5	0.3	28.0	1.6	25.5	1.6	29.2	0.3	0.1	0.1
TiO_2	37.30	0.49	37.67	0.30	34.69	3.54	34.85	0.72	1.92	1.59
Al_2O_3	1.12	0.08	0.96	0.05	5.26	6.08	2.38	0.26	0.38	0.11
Cr_2O_3	0.00	0.00	0.00	0.00	0.02	0.03	0.00	0.00	0.04	0.01
FeO	1.91	0.22	1.66	0.26	2.32	0.21	2.49	0.37	94.07	2.06
MnO	0.14	0.00	0.14	0.01	0.16	0.09	0.18	0.04	0.03	0.05
MgO	0.02	0.02	0.00	0.00	0.02	0.00	0.03	0.02	0.02	0.01
CaO	26.61	0.50	27.18	0.39	25.49	1.67	26.70	0.79	0.02	0.03
Na_2O	0.00	0.01	0.02	0.01	0.02	0.02	0.05	0.03	0.00	0.00
K_2O	0.00	0.00	0.00	0.00	0.00	0.00	0.00	0.00	0.00	0.00
Total	94.6		95.9		93.8		95.9		96.6	

compositional evolution. This may reflect a fractional crystallization trend (Yang et al. 2004b).

Plagioclase in GMS rocks commonly contains higher An component (An = 3–40), which is dominated by oligoclase, although albite and andesine are present (Table 3). Both inter- and intra-intrusion variations in plagioclase composition are evident: Lake George (An 26–40; Yang et al. 2002b), Tower Hill (3–12), Magaguadavic (13–29), and Bocabec Granite Suite (13–23). Importantly, the differences in the composition of plagioclase from phenocrysts (higher An) and groundmass (lower An component) in the same sample were noticed in the Lake George Granodiorite (Table 3 and eTable 3), reflecting the compositional evolution of magmas from which these plagioclase crystallized. Furthermore, chemical zoning reflected in the optical properties of plagioclase crystals are evident.

K-feldspar

Differences in the chemical composition of K-feldspar in GS and GMS rocks are evident, with a notable variation tendency (Table 3). In GS rocks, K-feldspar is mostly microcline, although microperthite and perthite occur in some of the intrusions (e.g., Mount Douglas Granite; see Cherry 1976; Cherry and Trembath 1978; McLeod 1990). Chessboard and (or) Carlsbad twinning are evident. Microcline is relatively pure (Or > 95), although some exceptions are present. Inter- and intra-intrusion variations in composition of microcline are noticeable (Table 3): the Mount Douglas ($Or_{81.8}Ab_{17.9}An_{0.3}$–$Or_{93.3}Ab_{6.4}An_{0.3}$), Beech Hill ($Or_{95.9}Ab_{4.0}An_{0.1}$), Sorrel Ridge ($Or_{88.7}Ab_{10.3}An_{1.0}$–$Or_{97.7}Ab_{2.2}An_{0.1}$), Pleasant Ridge Granites ($Or_{91.6}Ab_{8.3}An_{0.1}$–$Or_{96.9}Ab_{2.7}An_{0.4}$), Mount Pleasant ($Or_{98.4}Ab_{1.5}An_{0.1}$), and Kedron

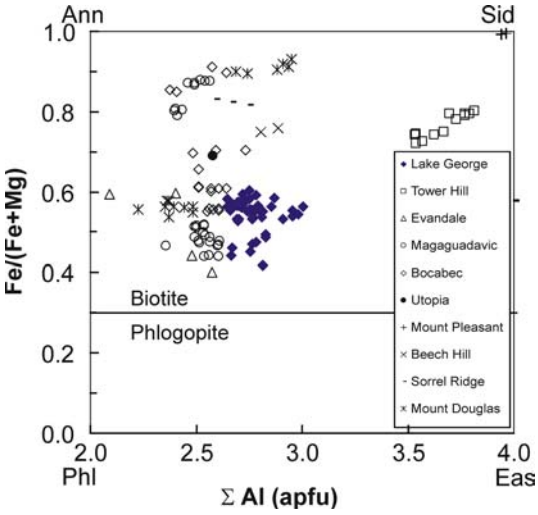

Fig. 3 Composition of biotite in granitoids from southwestern New Brunswick plotted on the Fe/(Fe + Mg) versus ΣAl (apfu) (apfu = atoms per formula unit) diagram, portrayed as the quadrilateral annite (*Ann*)—siderophyllite (*Sid*)—phlogopite (*Phl*)—eastonite (*Eas*) (after Rieder et al. 1998)

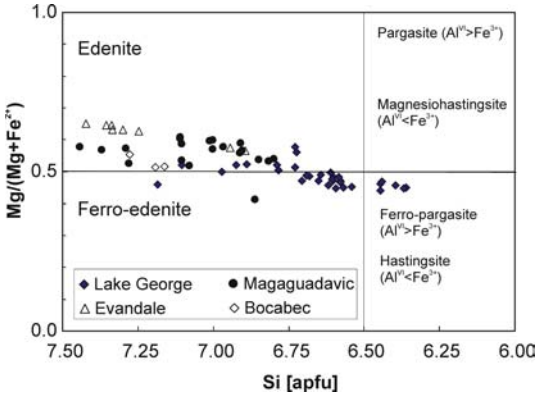

Fig. 4 Compositions of amphibole in granitoids from southwestern New Brunswick plotted in the amphibole classification diagram in terms of Si [apfu] versus Mg/(Mg + Fe^{2+}) by Leake et al. (1997). apfu = atoms per formula unit

($Or_{98.3}Ab_{1.7}An_{0.0}$–$Or_{98.7}Ab_{1.3}An_{0.0}$). This is also comparable to a trend of fractional crystallization.

In GMS rocks, K-feldspar is orthoclase to microcline, although microperthite and (or) perthite are evident. It appears that the range of variations in the composition of K-feldspar is larger for GMS rocks (Table 3). Similarly, inter-intrusion and intra-intrusion variations are present: the Lake George ($Or_{89.7}Ab_{10.0}An_{0.2}$ ~ $Or_{96.9}Ab_{3.0}An_{0.1}$; Yang et al. 2002b), Tower Hill ($Or_{91.5}Ab_{8.5}An_{0.0}$–$Or_{94.7}Ab_{5.1}An_{0.2}$), Magaguadavic ($Or_{72.9}Ab_{26.3}An_{0.80}$–$Or_{90.2}Ab_{9.5}An_{0.3}$), and Bocabec Granite Suite ($Or_{82.4}Ab_{17.3}An_{0.3}$–$Or_{94.2}Ab_{5.7}An_{0.1}$). Intra-intrusion variation in the chemical composition of K-feldspars may be interpreted by fractionation, whereas intra-intrusions are ascribed to the differences in sources, degrees of assimilation of wall rocks, and magmatic processes (Yang et al. 2004b).

Accessory minerals (excluding sulfides)

Representative EPMA determinations of accessory minerals are presented in Table 4. Garnet whose main components comprise almandine (66.1 ± 0.3 mol%) and spessartine (30.8 ± 0.3 mol%) occurs only in the marginal phase of the Tower Hill Granite intrusion, which resembles those from pegmatite, argillaceous metasediments, and (or) skarns (Deer et al. 1992).

Titanite is commonly present in GMS rocks, although it is also associated with chlorite and magnetite may be formed by hydrothermal alteration of hornblende and biotite (Fig. 2f) (Yang et al. 2002b). Euhedral titanite enclosed in hornblende is a primary phase in the Magaguadavic Granite Suite, displaying fairly consistent composition (Table 4).

Primary magnetite contains lower TiO_2in the Magaguadavic Granite Suite than those from the Bocabec Granite (Table 4), suggesting a different origin, although constant low TiO_2in magnetite may be ascribed to subsolidus recrystallization (cf. Keith et al. 1989). Subhedral and anhedral magnetite occur as alteration products of amphibole and biotite in the Lake George Granodiorite, with uncommon cubic grains found as inclusions in amphibole. Generally, magnetite is less abundant than ilmenite that occurs separately as subhedral and anhedral inclusions in biotite and amphibole (Yang et al. 2002b). Later ilmenite with higher MnO content (Table 4) also formed during the replacement of biotite, where it is usually distributed along the cleavage planes of the biotite, together with secondary chlorite or muscovite.

Apatite, zircon, and allanite occur in GMS rocks, whereas zircon, monazite, columbite, and xenotime commonly occur in GS granite. These minerals are not discussed further.

T–P-f_{O_2}- f_{HF}/f_{HCl} conditions

The mineral chemical data of rock-forming minerals in the granitoids described above (Table. 1, 2, and 3,) are used to constrain crystallization conditions, volatile exsolution, and fluorine-chlorine activity of fluids associated with these intrusions, and also to examine the degree of subsolidus reequilibration using various geothermobarometry techniques.

Temperatures

Hornblende-plagioclase geothermometry

Blundy and Holland (1990) established an empirical amphibole-plagioclase geothermometer based on edenite-tremolite reaction (i.e., edenite + 4 quartz = tremolite + albite), which can be used to estimate the temperature of quartz-bearing intermediate

Table 5 The results of temperature and pressure estimation

Intrusions	Sample	T_{Ab} (°C)	T_{Or}(°C)	T_{An} (°C)	$T_{Hb\text{-}Pl}$ (°C)	P_{Hb} (kb)
Mount Pleasant Granite Suite	AM96-3-1233	139	310	1559		
Beech Hill Granite	BH01-111	229	330	918		
Kedron Granite	BR84-4-87	146	239	2714		
	BR84-4-118	135	327	537		
	C81-9-258	291	271	3488		
	C81-10-209	252	248	2065		
	C81-10-289	326	192	5385		
Pleasant Ridge Granite	C82-4-14	182	252	7688		
	C82-5-75	308	268	2181		
Sorrel Ridge Granite	C80-9-137	298	413	1970		
	C80-10-353	177	419	714		
Mount Douglas Granite	85-197	335	587	709		
	85-218	483	461	704		
Lake George	LG78-18-1190	289	648	563		
	LG80-36-1647	368	668	342	772	4.6
		338 (G)[a]	544	551		
	LG81-2-1741	379	513	727	729	4.2
		288(G)	341	1727		
	LG81-12-1567	362	549	678		
		371(G)	516	585		
	LG81-14-1291	219	379	694		
	LG81-14-1886	308	480	1950		
	LG81-19-1351	243	466	526	731	4.6
	LG83-2-1995	429	555	580	740	3.4
	LG83-2-2461	407	595	592	742	4.5
Tower Hill Granite	C80-2-580	316	240	778		
	C80-5-279	254	283	1201		
	85-188	288	381	1255		
	85-214	274	348	939		
Evandale Granodirite	SEV01-125	329	438	473	617	0.6
Magaguadavic Granite Suite	85-186	360	451	1376		
	85-195	459	508	750	630	1.1
	85-196	413	492	630	650	1.5
	85-199	630	571	732		
Bocabec Granitoid Suite	85-176	357	494	795		
	85-178				600	2.8
	85-202	308	461	549		
	85-215	522	479	626		

[a]338 (G) denote plagioclase-K-feldspar pair occurring in groundmass in porphyritic granodirite

to felsic igneous rocks with plagioclase (An ≤ 0.92) and Si in amphibole (≤ 7.8 apfu). The geothermometer is described as the following formula.

$$T = \frac{0.677P[\text{kb}] - 48.98}{-0.0429 - 0.0083144 \ln\left\{\left(\frac{\text{Si}-4}{8-\text{Si}}\right)X_{\text{Ab}}^{\text{Pl}}\right\}}$$

where Si represents atoms per formula unit in amphibole and $X^{\text{Pl}}_{\text{Ab}}$ denotes the mole fraction of albite in plagioclase.

The samples from GMS rocks, such as the Lake George Granodiorite, Evandale Granite, Magaguadavic Granite Suite, and Bocabec Granitoid Suite (Table. 1 and 3) meet the requirements of this geothermometry. According to the equation, temperatures ($T_{\text{Hb-Pl}}$) calculated for cogenetic amphibole and plagioclase yield: 729–772°C for Lake George, ~617°C for Evandale, 630–650°C for Magaguaduavic, and ~600°C for Bocabec granitoids (Table 5). Godbout (1997) also used hornblende-plagioclase geothermomtry to estimate temperatures for granitoids from the Saint George Batholith. His results are: ~648°C for Evandale, ~645–676°C for Magaguaduavic, and ~700–746°C for Bocabec. His temperature estimates seemed to be higher for these intrusions. Therefore, except for the Lake George Granodiorite, these temperatures (Table 5) appear to be lower than the solidus of wet granodiorite and granite at 1–2 kb (Wyllie 1977; Whitney 1988).

Ternary feldspar thermometry

A practical spreadsheet program was compiled in this study in terms of the ternary feldspar thermometry (Fuhrman and Lindsley 1988), which was used to test for equilibration between plagioclase and alkali-feldspar in the Lake George Granodiorite (Yang et al. 2002b). When the chemical data (i.e., X_{Ab}, X_{Or}, and X_{An}) of plagioclase and K-feldspar (Table 3) are input into the program, the temperatures can be computed. The results indicate that T_{Ab} values are always lower than 500°C, consistent with the results using the calibration of Stormer (1975), although T_{Or} (350–668°C) and T_{An} (342–1,950°C) values are more varied. Similar results (i.e., $T_{\text{Ab}} \neq T_{\text{Or}} \neq T_{\text{An}}$) were also obtained for the other granitoid intrusions (Table 5). These demonstrate that magmatic equilibrations between plagioclase and

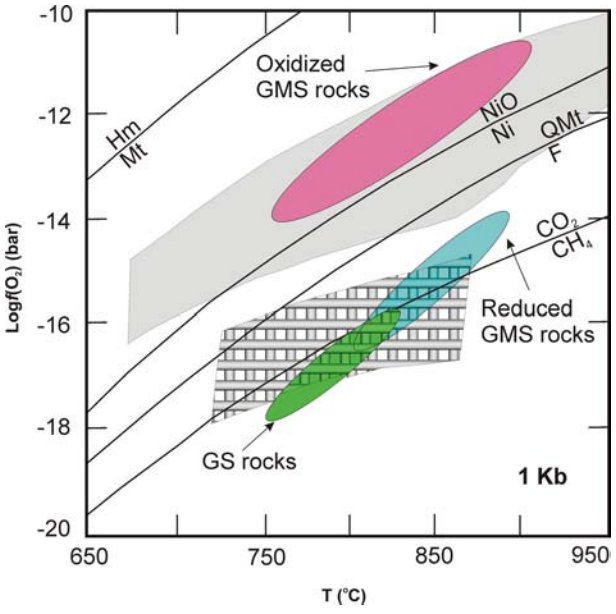

Fig. 5 Temperature versus oxygen fugacity diagram for southwestern New Brunswick granitoids. The *solid lines* show the f_{O_2}–T conditions for the redox buffers Hm-Mt (hematite and magnetite), NiO–Ni, Q–Mt–F (quartz, magnetite and fayalite), and CO_2–CH_4 (from Candela 1989). *Gray pattern* denotes weakly contaminated I-type (*I-WC*), moderately contaminated I-type (*I-MC*), and strongly contaminated I-type (*I-SC*); *chessboard pattern* represents strongly contaminated reduced I-type (*I-SCR*) granitoids (after Ague and Brimhall 1988). *Red area* represents the Magaguadavic Granite Suite and Bocabec Granitoid Suite (normal I-type); *Blue area* denotes granitoids from Lake George and Tower Hill (reduced I-type); *Green area* indicates the Beech Hill Granite, Sorrel Ridge Granite, Mount Pleasant Granite Suite and Mount Douglas Granite (fractionated I-type)

alkali-feldspar in granitoids may have been disturbed or may have not been maintained. These are interpreted as the effects of late-stage subsolidus hydrothermal processes, which have affected the feldspars and erased the records of original igneous equilibria. In this regard, Yang et al. (2004a) discussed the interaction between magmatic to hydrothermal fluids and the Lake George Granodiorite, which also affected oxygen and hydrogen isotopic equilibria among rock-forming minerals.

Pressures

Al-in-amphibole geobarometry (Hammarstrom and Zen 1986) has been widely used to estimate the pressures of igneous hornblende crystallization with the assemblage of quartz, plagioclase, orthoclase, biotite, amphibole, titanite, and ilmenite and (or) magnetite, which is suitable for GMS intrusions. The method has been tested with natural mineral and experimental data for pressures ranging from <1 to 10 kb (Rutter et al. 1989; see Stein and Dietl 2001 and references therein). For simplicity, this study uses the calibration of Hammarstrom and Zen (1986) to calculate pressures (P_{Hb}). The results (Table 5) indicate reasonable pressures for: the Evandale Granodiorite (~0.6 kb), the Magaguadavic Granite Suite (~1.1–1.5 kb), and the Bocabec Granitoid Suite (~2.8 kb), suggesting that hornblende began to crystallize in these intrusions at lower pressures than the Lake George Granodiorite stock (~3.4–4.6 kb) (Table 5; Yang et al. 2002b). Godbout (1997) obtained similar estimates, also based on the Al-in-hornblende geobarometry. In terms of textural characteristics, thickness of strata reconstruction, and the system Q-Ab-Or-H_2O phase diagram, the final emplacement pressures (P_{FE}) for these intrusions appear to be approximately ~1.5 kb for the Evandale Granodiorite, ~2.0–3.0 kb for Magaguadavic Granite Suite, and ~1 kb for Bocabec Granitoid Suite (Cherry 1976; McLeod 1990), and <2 kb for Lake George Granodiorite stock (Yang et al. 2002b).

Amphibole minerals are absent in GS rocks, thus the emplacement pressures of these intrusions are qualitatively estimated in terms of the rock textures, strata reconstruction, and the system Q-Ab-Or-H_2O phase diagram, which provided approximate pressures (P_{FE}) around 1 kb (Butt 1976; Cherry and Trembath 1978; Lentz and McAllister 1990; Lentz and Gregoire 1995).

Oxygen fugacity (f_{O_2})

The temperatures estimated from the rock-forming minerals of granitoids in this study reflect subsolidus processes, therefore, cannot represent the magmatic temperatures. Since T is a principal factor controlling the f_{O_2} in a system, appropriate T estimation is crucial in the determination of magmatic to hydrothermal redox conditions. Magma temperatures, however, may be estimated with zircon-, apatite-, and (or) monazite-saturation models experimentally determined for metaluminous to weakly peraluminous felsic melts (Watson and Harrison 1983; Harrison and Watson 1984; Montel 1993); the techniques yield three independent temperatures so that consistency can be checked. The results of temperature estimation using these models suggest that GMS rocks collectively have higher temperatures than GS rocks. Detailed information of temperatures is given in Yang et al. (2004b).

Granitoid oxygen fugacity (f_{O_2}) can be assessed from the Fe/(Fe + Mg) ratios of biotite (Table 2) associated with K-feldspar and magnetite in terms of the calibration of Wones and Eugster (1965) (see Wones 1980; Speer 1984; Lentz 1992, 1994). Temperatures are from Yang et al. (2004b); zircon-saturation temperatures that were consistent in the data set are used in the construction of Fig. 5. For reduced I-type granitoids, such as the Lake George Granodiorite, in which primary magnetite is absent, the calibration of Ague and Brimhall (1988) can be used to estimate their f_{O_2}. All the results are plotted in Fig. 5 and indicate that GS rocks and reduced GMS have lower values of f_{O_2} than those of normal I-type (oxidized) GMS rocks. For example, the values of f_{O_2} for the Lake George Granodiorite are be-

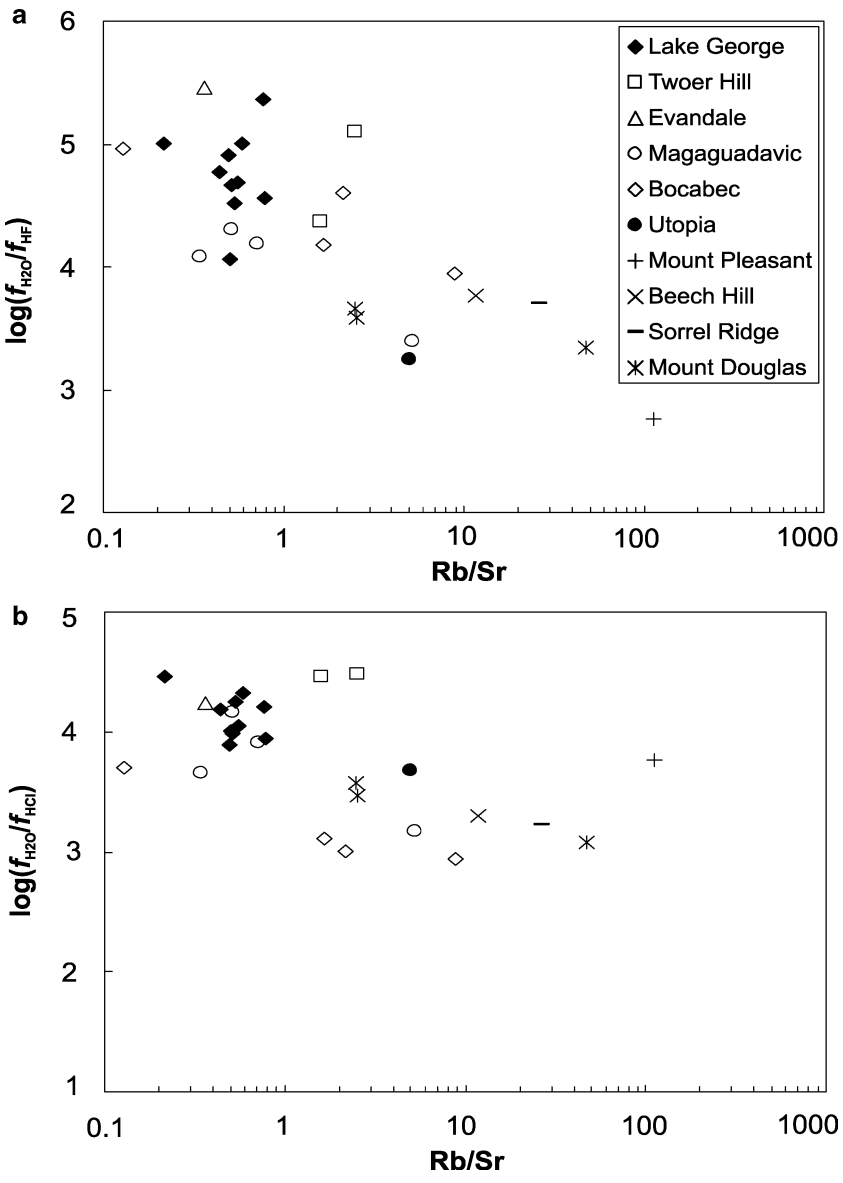

Fig. 6 Plot of Rb/Sr ratios against f_{H_2O}/f_{HF} (**a**) and f_{H_2O}/f_{HCl} ratios (**b**) in fluids in equilibrium with biotite from granitoids, southwestern New Brunswick. The Rb/Sr ratios of bulk rock data are from Yang et al. (2004), which increase with fractionation (cf. Keith et al. 1989). The calculations of f_{H_2O}/f_{HF} and f_{H_2O}/f_{HCl} ratios are based on the method of Munoz (1992); the average composition of biotite in the granitoid samples is from Table 2. Temperatures used in the calculations are the average zircon-saturation temperatures, which were given in Yang et al. (2004b): the Lake George Granodiorite 810°C, Tower Hill Granite 712°C, Evandale Granodiorite 833°C, Magaguadavic Granite Suite 821°C, Bocabec Granitoid Suite 933°C, Utopia Granite 777°C, Mount Pleasant Granite Suite 750°C, Beech Hill Granite 767°C, Sorrel Ridge Granite 750°C, and Mount Douglas Granite 770°C

tween $10^{-16.5}$ and $10^{-13.7}$ bars at "magmatic" temperatures, and for the Tower Hill Granite between $10^{-16.7}$ and $10^{-13.4}$ bars (Fig. 5), comparable with strongly contaminated reduced I-type granites (Ague and Brimhall 1988; Candela 1989). Interestingly, the f_{O_2} values of GS rocks (i.e., Sorrel Ridge, Beech Hill, Mount Pleasant, and Mount Douglas) are between $10^{-17.7}$~$10^{-15.8}$ bars (Fig. 5). However, oxidized I-type GMS rocks (i.e., the Magaguadavic Granite Suite, Bocabec Granitoid Suite) display high f_{O_2} values ranging from $10^{-14.0}$~$10^{-10.5}$ bars (Fig. 5), similar to weakly to moderately contaminated I-type granitoids elsewhere (Ague and Brimhall 1988; Candela 1989).

As it is known that GMS rocks from southwestern New Brunswick have comparable geochemical characteristics and thus have similar sources (Yang et al. 2004b), the difference in f_{O_2} for reduced and normal (oxidized) I-type granitoids observed in this study (Fig. 5) requires further discussion. The reduced I-type Lake George Granodiorite stock intruded Kingsclear Group metasedimentary sequence containing reduced organic-carbon (Seal et al. 1987; Yang et al. 2002b), which may result in assimilation plus interaction with circulation of hydrothermal systems (bearing CO_2–CH_4) driven by the intrusion (Yang et al. 2004a). In the Bocabec Granitoid Suite, a granitoid intruded a gabbro body that contains appreciable magnetite, however, retains its high redox condition. This oxidized state is also reflected in the assemblage of magnetite + titanite + quartz in the granitoid (cf. Wones 1989). Therefore, local redox buffers in the country rocks may play an important role in affecting the oxidation state of granitoid intrusions and indirectly control the genesis of intrusion-related gold systems.

Granitic series rocks, exhibiting lower redox than GMS rocks, may reflect their different petrogenesis as is

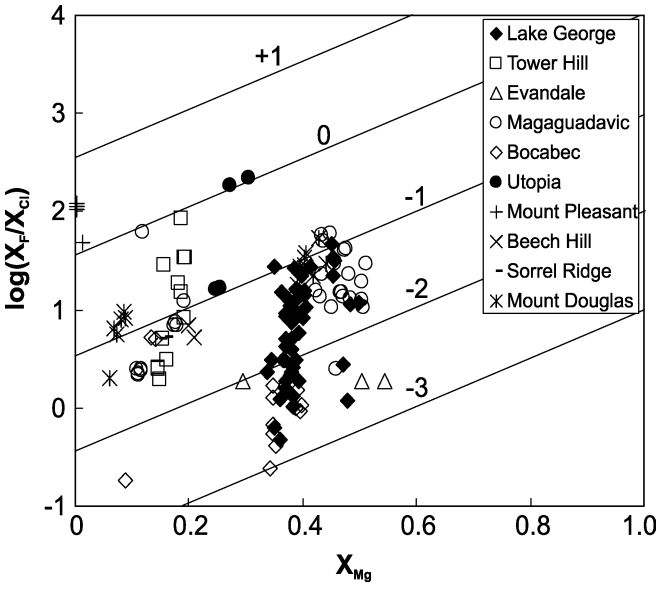

Fig. 7 X_{Mg} versus $\log(X_F/X_{Cl})$ of biotite from granitoids, southwestern New Brunswick. X_F and X_{Cl} are the mole fractions of F and Cl in the hydroxyl site, respectively. Contours are the logarithm of the fluorine-chlorine fugacity ratios (f_{HF}/f_{HCl}) for a fluid in equilibrium with biotite (Munoz 1992), calculated at 400°C

also shown in their distinctive geochemistry (Yang et al. 2004b). Yang et al. (2004b) suggested that GS granites might have been derived in part from partial melting of quartzofeldspathic rocks (igneous) within the crust (i.e., their source region may be above that of GMS rocks), and then the magmas may have experienced extensive fractionation. Thus, source control on redox may be important for GS rocks.

The conditions of f_{HF}/f_{HCl} in fluids evolved from the granitoids

Although the hydroxyl site of biotite is susceptible to Cl–OH exchange during its interaction with hydrothermal fluids, the systematics of F, Cl, and OH are useful for qualitatively inferring the relative HF, HCl, and H_2O fugacities of volatiles associated with felsic melts (Munoz and Swenson 1981; Munoz 1984, 1992; Keith and Shanks 1988; Keith et al. 1989; van Middelaar and Keith 1990; Zhu and Sverjensky 1991; Lentz 1992, 1994; Coulson et al. 2001; Yang 2002b). Figure 6 presents the relationships between bulk rock Rb/Sr ratios and calculated f_{H_2O}/f_{HF} and f_{H_2O}/f_{HCl} ratios in fluids evolved from the granitoids. The calculations of f_{H_2O}/f_{HF} and f_{H_2O}/f_{HCl} ratios are based on the revised equations of Munoz (1992). Less evolved GMS rocks display relatively higher f_{H_2O}/f_{HF} ratios, whereas highly fractionated GS rocks have lower f_{H_2O}/f_{HF} ratios (Fig. 6a). The f_{H_2O}/f_{HF} ratios appear to decline with fractionation for both GMS and GS rocks. The f_{H_2O}/f_{HCl} ratios are more consistent (Fig. 6b), although the ratios also decline with fractionation.

On the diagram of the mole fraction X_{Mg} in the octahedral site versus $\log(X_F/X_{Cl})$ of biotite (Fig. 7) where X_F and X_{Cl} are respectively the mole fraction of F and Cl in the hydroxyl site, biotite has a significant range of $\log(X_F/X_{Cl})$ ratios for particular intrusions, reflecting these biotite may have been interacted with subsolidus hydrothermal fluids. For example, the large range of calculated halogen fugacity ratios [$\log(f_{HF}/f_{HCl}) = -3$ to -1, at 400°C] for magmatic fluids in equilibrium with biotite in the Lake George Granodiorite, suggests that the halogens in biotite might have been reequilibrated with various Cl-rich magmatic fluids (Fig. 7). These fluids probably emanated from the crystallizing granodiorite magma at depth and differentially partitioned the volatiles and solutes from that magma during progressive crystallization. The data illustrated in Fig. 7 also indicate that either the biotite compositions represent a crystallization sequence, an unreasonable conclusion for the Lake George Granodiorite, or that the biotite has been reequilibrated with orthomagmatic to exogenetic fluids of variable composition (i.e., those with different f_{HF}/f_{HCl} ratios). If magmatic, these fluids could have changed with time as the magma cooled and solidified at depth, such that the f_{HF}/f_{HCl} ratios of the fluids would progressively increase (Fig. 7).

Biotite in the Tower Hill Granite has lower values of X_{Mg} (0.15–0.20) than those in the Lake George Granodiorite (Table 1, Fig. 7), but seemed to have equilibrated with a fluid with relatively higher $\log(f_{HF}/f_{HCl})$ ratios ($-1.5 \sim -0.1$, at 400°C). The Magaguadavic Granite Suite contains two groups of biotite, i.e., high X_{Mg} and low X_{Mg} ones, although the calculated $\log(f_{HF}/f_{HCl})$ ratios in fluids associated with these biotite are mostly confined between -1 and -2 (Table 2, Fig. 7). Notably, in the Bocabec Granitoid Suite biotite with high X_{Mg}values have equilibrated with a fluid with low $\log(f_{HF}/f_{HCl})$ ratios ($-3 \sim -2$), whereas those with low X_{Mg} values equilibrated with fluids having higher $\log(f_{HF}/f_{HCl})$ ratios ($-1.5 \sim -1.0$).

Biotite in GS rocks commonly has low X_{Mg} values (Table 2), and the fluids associated with these biotite minerals normally display relatively high $\log(f_{HF}/f_{HCl})$ ratios ($-1.5 \sim +0.5$) (Fig. 7). It is noted that the Mount Douglas Granite has biotite with high X_{Mg} values (0.40~0.42), but the calculated $\log(f_{HF}/f_{HCl})$ ratios ($\sim -1.5 \sim -0.7$) in related fluid are similar to those with low X_{Mg} values (~0.06–0.10) (Fig. 7). This indicates the fluids associated with the Mount Douglas Granite intrusion remain relatively constant in f_{HF}/f_{HCl} ratios through fractionation.

Estimate of water contents in granitoid melts

Several lines of evidence from petrography suggest the GMS and GS granitoids are saturated with water prior to the final solidification (see the section of petrogra-

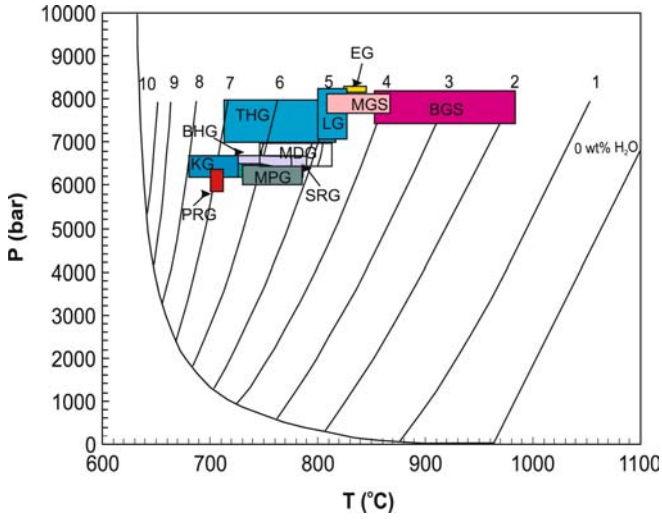

Fig. 8 Estimate of water contents (wt% H_2O) in the initial granitoid melts for granitoid intrusions from southwestern New Brunswick, based on the model of Holtz et al. (2001). GMS rocks contain less water than the GS rocks. The intrusion labels as Fig. 1

phy; Yang et al. 2002b, 2004a, b). However, this does not necessarily mean that the initial melts of these granitoids are water-saturated (Burnham 1979; Burnham and Ohmoto 1980; Candela 1989, 1997; Keith et al. 1989; Scaillet et al. 1998; Clemens and Watkins 2001; Holtz et al. 2001). In fact, the formation of most granitoid melts by partial melting reaction during upper amphibolite-to granulite-grade metamorphism within crust generally occurs in the absence of excess pervasive fluids (see Clemens and Watkins 2001; Thompson 2001). Decompression and crystallization of anhydrous minerals result in water saturation in granitoid melts (cf. Burnham 1979; Candela 1989, 1997), which is essential for generating magmatic hydrothermal (possibly mineralizing) fluids (cf. Burnham and Ohmoto 1980). The water contents of initial felsic melts may have controlled the final water saturation of the pertinent granitoid intrusions, and sufficiently affected viscosity of the melts, which may have controlled the ability of melts to segregate from the source area and to migrate through the crust (Holtz et al. 2001 and references therein). Water solubility in felsic melts is a function of P, T, X, and water activity (Burnham 1979; Holtz et al. 2001 and references therein), which can be estimated by the method recently developed by Holtz et al. (2001). Assuming GMS rocks derived from the deeper lower crust than GS intrusions and using zircon-saturation temperatures of the least-evolved phases in each intrusion and (or) suite to represent their initial liquidus temperatures (Yang et al. 2004b), the minimum water contents of the granitoid melts can be obtained (Fig. 8).

Granodioritic to monzogranitic series intrusions contain less water in their initial melts compared to GS intrusion (Fig. 8). The water contents in the initial melts approximately vary from the Bocabec Granitoid Suite (~2–4 wt%) through Magaguadavic Granite Suite (~4–5 wt%), Evandale Granodiorite (~4.5 wt%), Lake George Granodiorite (~ 4.5–5 wt%) to the Tower Hill Granite (~5–7 wt%).

Granitic series intrusions have relatively higher water concentrations in their initial melts, which displays a systematic increase from the Mount Douglas Granite (~4.5–6.2 wt%) through Sorrel Ridge Granite (~5–6.4 wt%), Beech Hill Granite (~5.5–6.3 wt%) to Pleasant Ridge Granite (~6.6–7.2 wt%) and Kedron Granite (~6.5–8.0 wt%). Given adiabatic decompression, a significant amount of water can be released from these intrusions (Fig. 8), particularly for GMS intrusions, as they fall into the field with more gentle slopes of liquidus curves.

Discussion

Evidence from this study and petrochemistry (Yang et al. 2004b) reveals the differences between GS and GMS granitoids in southwestern New Brunswick, suggesting that these are distinct aspects of their origin, petrogenetic processes, crystallization history, exsolution of fluids, fluid chemistry, and associated mineralization. Textures and mineral assemblages are direct features to qualitatively display the emplacement levels and cooling history of these intrusions. GS granite intrusions demonstrate high level features (≤ 1 kb), whereas GMS granitoids have variable levels of emplacement ranging from > 3 kb (e.g., Tower Hill Granite; Butt 1976) to ~1 kb (e.g., the Bocabec Granitoid Suite; Cherry 1976; McLeod 1990). Estimates from Al-in-hornblende geobarometry reveals that the onset of hornblende crystallization in the various GMS intrusions changes (Table 5), implying that these magmas have intrinsically different original water activities (see Candela 1997), which affects the timing of water-saturation. This is consistent with the results (Fig. 8) estimated from the model of Holtz et al. (2001). Water might be saturated in the Lake George Granodiorite and Bocabec Granitoid Suite before their final emplacement (i.e., $P_{Hb} > P_{FE}$), whereas water began to be saturated in the Magaguadavic Granite Suite and Evandale Granodiorite after their emplacement (i.e., $P_{Hb} < P_{FE}$).

Ternary feldspar geothermometry (Fuhrman and Lindsley 1988) can be used to test magmatic equilibration between plagioclase and K-feldspar in both GS and GMS granitoid rocks. The inconsistency of $T_{Ab} \neq T_{Or} \neq T_{An}$ (see Table 5) suggests that the igneous signatures are disturbed by subsolidus and (or) late stage hydrothermal fluids (cf. Martin 1988; Yang et al. 2002b). Although the amphibole-plagioclase geothermometer (Blundy and Holland 1990) is contentious (Hammarstrom and Zen 1992; Poli and Schmidt 1992; Rutherford and Johnson 1992), it is able to produce reasonable temperatures, if the requirements of the geothermometer are met (Stein and Dietl 2001). Its

application to the Lake George Granodiorite also yielded reasonable temperature estimates (Table 5). However, relatively lower temperatures for the other GMS intrusions (Table 5) may be ascribed to the interaction of hornblende and plagioclase with hydrothermal fluids. Holland and Blundy (1994) revised their amphibole-plagioclase geothermometer, taking into consideration all components involved in the edenite-tremolite reaction. The revised equations were tested by Stein and Dietl (2001) and produced temperatures 30∼70°C lower than those of the original calibration, but with significantly larger errors.

Biotite chemistry has been widely used to infer the origin of granitoids, magmatic to hydrothermal processes and related f_{O_2}, f_{HF}/f_{HCl} ratios, relationships to metal mineralization, and even tectonic setting (Wones and Eugster 1965; Wones 1980, 1989; Munoz and Swenson 1981; Munoz 1984, 1992; Speer 1984; Ague and Brimhall 1988; Keith and Shanks 1988; Candela 1989; Keith et al. 1989; van Middlelaar and Keith 1990; Lentz 1992, 1994; Lalonde and Bernard 1993; Müller and Groves 1993, 2000; Abdel-Rahman 1994; Coulson et al. 2001; Shabani et al. 2003; references therein). Based on the biotite discrimination diagram of Abdel-Rahman (1994), these biotite are mostly located in calc-alkaline and peraluminous fields, consistent with the petrochemical study (Yang et al. 2004b). Shabani et al. (2003) dealt with a large database of biotite in granitoids from the Canadian Appalachians; they also obtained a similar result for biotite in calc-alkaline and peraluminous southwestern New Brunswick granitoids and emphasized supracrustal assimilation in their petrogenesis. Importantly, most biotite (Table 1) in southwestern New Brunswick granitoids fall into the "mineralized" field on the F (wt%) versus Cl (wt%) diagram of Müller and Groves (2000), suggesting that these granitoids are prospective for gold mineralization.

The Cl–OH and F–OH exchange in the hydroxyl site of biotite is susceptible to interaction with hydrothermal fluids, which may impact cations in the octahedral sites given the presence of correlation between (F–Cl–OH) and (Al + Ti + Fe^{3+} + Cr) (see Righter et al. 2002). Therefore, more precise techniques (Righter et al. 2002) are needed to determine H_2O content and Fe^{2+}/Fe^{3+} ratios in biotite, in order to obtain detailed genetic information from biotite chemistry. Although this is true, varying ranges of X_{Mg} and X_F/X_{Cl} in biotite from GMS and GS granitoids (Fig. 7) are evident, suggesting that their source, petrogenetic processes, and associated fluids are different. Relatively high f_{HCl}/f_{HF} ratios in fluids associated with GMS granitoid intrusions may be important to the genesis of intrusion-related gold systems. Coulson et al. (2001) suggested that gold-related granitoid within the Emerald Lake pluton (Yukon Territory) is associated with magmatic fluids of high chlorine activity. These provide a probable connection for gold as chloride complexes in magmatic fluids. As pointed out by Gammons and Williams-Jones (1997), high temperature Cl-rich fluids can effectively transport gold, consistent with the investigations of high T experiments (Hayashi and Ohomoto 1991; Frank et al. 2002) and numerous empirical observations from gold deposits (see McCoy et al. 1997; Müller and Groves 2000; Groves et al. 2003 and references therein). As temperature decreases, gold is mainly transported as bisulfide complexes in fluids and may be precipitated at shallower levels in an epithermal setting (Hayashi and Ohomoto 1991; Richards 1995; Gammons and Williams-Jones 1997).

Redox conditions of granitoid intrusions and associated hydrothermal systems are essential for the origin of intrusion-related gold systems (McCoy et al. 1997; Thompson et al. 1999; Lang et al. 2000; Thompson and Newberry 2000; Baker 2002; Lang and Baker 2001; Bierlein et al. 2003; Fan et al. 2003; Groves et al. 2003; Doebrich et al. 2004). Redox buffer from the country rock is important for affecting the oxidation states of granitoid intrusions. Reduced organic-carbon in black shale and graphite-bearing slate is a critical redox buffer for a cooling granitoid intrusion. Assimilation plus circulation of hydrothermal systems driven by the intrusion may transform an oxidized arc-magma to a relatively reduced I-type granite (see Ague and Brimhall 1988), i.e., ilmenite as the dominant Fe–Ti oxide in the granitoids. Fox-red biotite in reduced GMS granitoid intrusions, such as the Lake George Granodiorite (Yang et al. 2002b), is a good indicator of redox. Ishihara (1981) proposed that organic carbon in the source region placed the most important control on the redox condition of granitoids. However, the control of local country rocks on oxidation state of a cooling granite intrusion and (or) suite is also important, given that arc-like calc-alkaline, metaluminous to weakly peraluminous magmas (I-type) are typically characterized by high redox conditions. The differences in redox condition reflected by the mineral assemblages from different I-type granitoid intrusions of similar ages in the region must have been controlled by the distinctive country rocks having different redox buffers (e.g., reduced organic carbon versus magnetite or hematite). Therefore, this study suggests that local redox controls play an important role in intrusion-related gold systems.

Conclusions

In southwestern New Brunswick, Late Devonian GS granites (fractionated I-type) and Late Silurian to Early Devonian GMS granitoids (I-type) display distinctive characteristics of petrology and mineralogy, suggesting differences in their petrogenesis. This is manifested in the intensive variables of granitoid magmas and associated hydrothermal fluids, such as temperature, pressure, water activity, oxygen fugacity, and fluorine-chlorine activity. "Water rich" GS granite melts are formed at relatively lower temperatures at relatively shallower levels of the crust, whereas "water poor" GMS granitoids are generated at higher temperatures at relatively deeper

levels. However, a significant amount of water may have emanated from GMS intrusions during their final emplacement at upper crust levels as they fall into the field with gentle slope of liquidus curves, and thus produce magmatic fluids that may have potential for generating mineralization of gold and (or) related metals.

Magmatic equilibrium among rock-forming minerals in both GS and GMS granitoids may have been disturbed by subsolidus and (or) late stage hydrothermal fluids. These fluids display variable f_{HF}/f_{HCl} ratios and may result from sequential emanations from progressively cooling magmas at depth. The fluids associated with GS intrusions commonly have higher f_{HF}/f_{HCl} ratios ($10^{-1.4}\sim10^{0.5}$) than GMS granitoid intrusions ($10^{-3.0}\sim10^{-1.0}$). Within a granitoid suite, f_{HF}/f_{HCl} ratios usually increase with fractionation, consistent with the decrease in f_{H_2O}/f_{HF} greater than f_{H_2O}/f_{HCl} ratios with fractionation (Fig. 6). Magmatic fluids associated with GMS granitoids have relatively lower f_{HF}/f_{HCl}, which imply that gold may be transported as chloride complexes in Cl-rich fluids at high T.

Evolved I-type GS granites are characterized by reduced features, thus exhibiting lower f_{O_2} ($10^{-17.7}\sim10^{-15.8}$ bars) than GMS granitoids. GMS granitoid intrusions display two groups regarding f_{O_2} (i.e., reduced $10^{-16.7}\sim10^{-13.4}$ bars, and oxidized $10^{-14.0}\sim10^{-10.5}$ bars), which is interpreted as that these intrusions are intruded into distinctive country rocks that act as redox buffers. Local redox conditions (i.e., reduced setting owing to the presence of reduced organic-carbon or graphite in the country rocks) play a key part in the genesis of intrusion-related gold systems. Fox-red biotite is a petrographic indicator for reduced I-type GMS granitoids, which is significant for the exploration of intrusion-related gold systems.

Acknowledgements We are grateful to Dr. D.C. Hall (UNB) for assistance in EPMA analysis, Dr. Steve McCutcheon (New Brunswick Department of Natural Resources) for discussions on regional and local geology, and Dr. Joseph B. Whalen (Geological Survey of Canada, Ottawa) for providing his archived samples. We thank the journal reviewers Dr. Jeffrey D. Keith and Dr. A.F. Abdel-Rahman for their constructive comments. Prof. Dr. J. Hoefs is thanked for editorial handling of this paper. This study was funded by a Discovery grant from Natural Sciences and Engineering Research Council of Canada to DRL, with partial support from New Brunswick Innovation Fund, the New Brunswick Department of Natural Resources, and the Geological Survey of Canada—Targeted Geoscience Initiative program (GSC-TGI, 010008).

References

Abdel-Rahman AF (1994) Nature of biotites from alkaline, calc-alkaline, and peraluminous magmas. J Petrol 25:525–541

Ague JJ, Brimhall GH (1988) Regional variations in bulk chemistry, mineralogy and the compositions of mafic and accessory minerals in the batholiths of California. Geol Soc Am Bull 100:891–911

Baker T (2002) Emplacement depth and carbon dioxide-rich fluid inclusions in intrusion-related gold deposits. Econ Geol 97:1111–1117

Barr SM, White CE (1999) Field relations, petrology, and structure of Neoproterozoic rocks in the Caledonian Highlands, southern New Brunswick, Canada. Geological Survey of Canada Bulletin 530, 101 pp

Bierlein FP, Whitam R, McKnight S, Dodd R (2003) Intrusive-related gold systems in the western Lachlan Orogen, SE Australia. In: Eliopoulos DG (eds) Mineral exploration and sustainable development. Millpress, Rotterdam, pp 239–242

Blundy JD, Holland TJB (1990) Calcic amphibole equilibria and a new amphibole-plagioclase geothermometer. Contrib Mineral Petrol 104:208–224

Burnham CW (1979) Magmas and hydrothermal fluids. In: Barnes HL (ed) Geochemistry of hydrothermal ore deposits, 2nd edn. Wiley, New York, pp 71–136

Burnham CW, Ohmoto H (1980) Late-stage processes of felsic magmatism. Mining Geol Spec Issue 8:1–11

Butt KA (1976) Genesis of granitic stocks in southwestern New Brunswick. Unpublished PhD thesis, University of New Brunswick, Fredericton, 235 pp

Candela PA (1989) Felsic magmas, volatiles, and metallogenesis. In: Whitney JA, Naldrett AJ (eds) Ore deposition associated with magmas. Rev Econ Geol 4:223–233

Candela PA (1997) A review of shallow, ore-related granites: textures, volatiles, and ore metals. J Petrol 38:1619–1633

Candela PA, Piccoli PM (1995) Model ore-metal partitioning from melts into vapor and vapor/brine mixtures. In: Thompson JFH (ed) Magmas, fluids, and ore deposits. Mineralogical Association of Canada Short Course Series, vol 23, pp 101–127

Cherry ME (1976) The petrogenesis of granites in the St. George Batholith, southwestern New Brunswick, Canada. Unpublished PhD Thesis, University of New Brunswick, Fredericton, 242 pp

Cherry ME, Trembath LT (1978) Structural state and composition of alkali feldspars in granites of the St. George pluton, southwestern New Brunswick. Mineral Mag 42:391–399

Chi G (2002) Fluid compositions and temperature-pressure conditions of intrusion-related gold systems in southwestern New Brunswick—a fluid inclusion study. Geological Survey of Canada, Current Research 2002-E13:1–11

Clemens JD, Vielzeuf D (1987) Constraints on melting and magma production in the crust. Earth Planet Sci Lett 86:287–306

Clemens JD, Watkins JM (2001) The fluid regime of high temperature metamorphism during granitoid magma genesis. Contrib Mineral Petrol 140:600–606

Coulson IM, Dipple GM, Raudsepp M (2001) Evolution of HF and HCl activity in magmatic volatiles of the gold-mineralized Emerald Lake pluton, Yukon Territory, Canada. Mineralium Deposita 36:594–606

Davis WJ, Chi G, Castonguay S, McLeod M (2004) Temporal relationships between plutonism, metamorphism, and gold mineralization in southwestern New Brunswick: U-Pb and $^{40}Ar/^{39}Ar$ geochronological constraints. Geological Survey of Canada, Current Research 2004-F2:1–20

Deer WA, Howie RA, Zussman J (1992) An introduction to the rock-forming minerals. Essex, Longman, 696 pp

Doebrich JL, Zahony SG, Leavitt JD, Portacio JSJr, Siddiqui AA, Wooden JL, Fleck RJ, Stein HJ (2004) Ad Duwayhi, Saudi Arabia: geology and geochronology of a Neoproterozoic intrusion-related gold system in the Arabian Shield. Econ Geol 99:713–741

Fan HR, Zhai MG, Xie YH, Yang JH (2003) Ore-forming fluids associated with granite-hosted gold mineralization at the Sanshandao deposit, Jiaodong gold province, China. Mineralium Deposita 38:739–750

Frank MR, Candela PA, Piccoli PM, Glascock MD (2002) Gold solubility, speciation, and partitioning as a function of HCl in the brine-silicate melt-metallic gold system at 800°C and 100 MPa. Geochimica Cosmochimica Acta 66:3719–3732

Fuhrman ML, Lindsley DH (1988) Ternary-feldspar modeling and thermometry. Am Mineral 73:201–215

Fyffe LR, Fricker A (1987) Tectonostratigraphic terrane analysis of New Brunswick. Maritime Sediments Atl Geol 23:113–122

Fyffe LR, Pickerill RK, Stringer P (1999) Stratigraphy, sedimentology and structure of the Oka Bay and Waweig formations, Mascarene Basin: implications for the paleotectonic evolution of the southwestern New Brunswick. Atl Geol 35:59–84

Gammons CH, Williams-Jones AE (1997) Chemical mobility of gold in the porphyry-epithermal environment. Econ Geol 92:45–59

Godbout J (1997) Application of the Al-in-hornblende geobarometer and the hornblende-plagioclase geothermometer to the St. George Batholith, in SW New Brunswick. Unpublished BSc Thesis, University of New Brunswick, Fredericton, 65 pp

Groves DI, Goldfarb RJ, Robert F, Hart CJR (2003) Gold deposits in metamorphic belts: overview of current understanding, outstanding problems, future research, exploration significance. Econ Geol 98:1–29

Gunow AJ, Ludington S, Munoz JL (1980) Fluorine in micas from the Henderson molybdebite deposit, Colorado. Econ Geol 75:1127–1137

Hammarstrom JM, Zen E-an (1986) Aluminium in hornblende: an empirical igneous geobarometer. Am Mineral 71:1297–1313

Hammarstrom JM, Zen E-an (1992) Discussion of Blundy and Holland's (1990) Calcic amphibole equilibria and a new amphibole-plagioclase geothermometer. Contrib Mineral Petrol 111:264–266

Harrison TM, Watson EB (1984) The behavior of apatite during crustal anatexis: equilibrium and kinetic considerations. Geochimica Cosmochimica Acta 48:1467–1477

Hayashi KI, Ohomoto H (1991) Solubility of gold in NaCl- and H_2S-bearing aqueous solutions at 250–350°C. Geochimica Cosmochimica Acta 55:2111–21226

Holland TJB, Blundy JD (1994) Non-ideal interactions in calcic amphiboles and their bearing on amphibole-plagioclase thermometry. Contrib Mineral Petrol 116:433–447

Holtz F, Johannes W, Tamic N, Behrens H (2001) Maximum and minimum water contents of granitic melts generated in the crust: a reevaluation and implications. Lithos 56:1–14

Ishihara S (1981) The granitoid series and mineralization. Economic Geology 75th Anniversary Issue, pp 458–484

Keith JD, Shanks WC (1988) Chemical evolution and volatile fugacities of the Pine Grove porphyry molybdenum and ash-flow tuff system, southwestern Utah. In: Taylor RP, Strong DF (eds) Recent advances in the geology of granite-related mineral deposits. Canadian Institute of Mining and Metallurgy, Special vol 39, pp 402–423

Keith JD, van Middelaar W, Clark AH, Hodgson CJ (1989) Granitoid textures, compositions, and volatile fugacities associated with the formation of tungsten-dominated skarn deposits. In: Whitney JA, Naldrett AJ (eds) Ore deposition associated with magmas. Rev Econ Geol 4:235–250

Keith JD, Christiansen EH, Maughan DT, Waite KA (1998) The role of mafic alkaline magmas in felsic porphyry-Cu and Mo systems. In: Lentz DR (ed) Mineralized intrusion-related skarn systems. Mineralogical Association of Canada Short Course Series 26, pp 211–244

Kirkham RV, Sinclair WD (1988) Comb quartz layers in felsic intrusions and their relationship to porphyry deposits. In: Taylor RP, Strong DF (eds) Recent Advances in the Geology of Granite-Related Mineral Deposits, Canadian Institute of Mining and Metallurgy, Special vol 39, pp 50–71

Lalonde AE, Bernard P (1993) Composition and color of biotite from granites: two useful properties in the characterization of plutonic suites from the Hepburn internal zone of Wopmay orogen, Northwest Territories. Can Mineral 31:203–217

Lang JR, Baker T (2001) Intrusion-related gold systems: the present level of understanding. Mineralium Deposita 36:477–489

Lang JR, Baker T, Hart CJ, Mortensen JK (2000) An exploration model for intrusion-related gold systems. Soc Econ Geol Newslett 40:1–15

Le Maitre RW, Streckeisen A, Zanettin B, Le Bas MJ, Bonin B, Bateman P, Bellieni G, Dudek A, Efremova SA, Keller J, Lameyre J, Sabine PA, Schmid R, Sørensen H, Woolley AR (2002) Igneous rocks: a classification glossary of terms. Cambridge University Press, Cambridge, 236 pp

Leake BE, Woolley AR, Arps CES, Birch WD, Gilbert MC, Grice JD, Hawthorne FC, Kato A, Kisch H, Krivovivhev VG, Linthout K, Laird J, Mandarino JA, Maresch WV, Nickel EH, Rock NMS, Schumacher JC, Smith DC, Stephenson NCN, Ungaretti L, Whittaker EJW, Guo Y (1997) Nomenclature of amphiboles: report of the Subcommittee on Amphiboles of the International Mineralogical Association, Commission on New Minerals and Mineral Names. Am Mineral 82:1019–1037

Lentz DR (1992) Petrogenesis and geochemical composition of biotites in rare-element granitic pegmatites in the southwestern Grenville Province, Canada. Minerals Petrol 46:239–256

Lentz DR (1994) Exchange reactions in hydrothermally altered rocks: examples from biotite-bearing assemblages. In: Lentz DR (ed) Alteration and alteration processes associated with ore-forming systems. Geological Association of Canada Short Course Notes 11, pp 69–99

Lentz DR, Fowler AD (1992) A dynamic model for graphic quartz-feldspar intergrowths in granitic pegmatites in the southwestern Grenville Province. Can Mineral 30:571–585

Lentz DR, Gregoire C (1995) Petrology and mass-balance constraints on major-, trace-, and rare-earth-element mobility in porphyry-greisen alteration associated with the epizonal True Hill granite, southwestern New Brunswick, Canada. J Geochem Explor 52:303–331

Lentz DR, McAllister AL (1990) The petrogenesis of tin- and sulfide-lode mineralization at True Hill, southwestern New Brunswick. Atl Geol 26:139–155

Lentz DR, Thorne KG, Yang XM (2002) Preliminary analysis of the controls on the various episodes of gold mineralization at the Lake George antimony deposit, New Brunswick. In: Carroll BMW (ed) Current Research 2002, New Brunswick Department of Natural Resources and Energy Division, Mineral Resource Report 02–1, pp 55–79

Martin RF (1988) The K-feldspar mineralogy of granites and rhyolites: a generalized case of pseudomorphism of the magmatic phase. Rendiconti Della Società Italiana Di Mineralogia e Petrologia 43:343–354

McCoy D, Newberry RJ, Layer P, DiMarchi JJ, Bakke A, Masterman JS, Minehane DL (1997) Plutonic-related gold deposits of Interior Alaska. Econ Geol Monogr 9:191–241

McCutcheon SR, Sinclair WD, Kooiman GJA (2001) The Late Devonian Mount Pleasant Caldera: geological setting of a W-M0-Sn-In deposit in southwestern New Brunswick. In: Pickerill R, Lentz DR (eds) Guidebook to field trips in New Brunswick and western Maine, 93rd Annual Meeting New England Intercollegiate Geological Conference, pp B5–B14

McLeod MJ (1990) Geology, geochemistry, and related mineral deposits of the Saint George Batholith; Charlotte, Queens, and Kings Counties, New Brunswick. New Brunswick Department of Natural Resources and Energy, Mineral Resources, Mineral Resource Report 5, 169 pp

McLeod MJ, Fyffe LR (2002) Geology and gold occurrences, Clarence Stream area, southwestern New Brunswick. New Brunswick Department of Natural Resources and Energy; Minerals, Policy and Planning Division, Plate 38A

McLeod MJ, McCutcheon SR (2000) Gold environments in New Brunswick. New Brunswick Department of Natural Resources and Energy, Minerals and Energy Division, Map Plate 2000–8

McLeod MJ, Johnson SC, Ruitenberg AA (1994) Geological map of southwestern New Brunswick. New Brunswick Department of Natural Resources and Energy, Mineral Resources, Map NR-5

van Middlelaar WT, Keith JD (1990) Mica chemistry as an indicator of oxygen and halogen fugacities in the CanTung and other W-related granitoids in the North American Cordillera. In: Stein HJ, Hannah JL (eds) Ore-bearing granite systems; petrogenesis and mineralizing processes. Geological Society of America Special Paper 246, pp 205–220

Miller BV, Fyffe LR (2002) Geochronology of the Letete and Waweig formations, Mascarene Group, southwestern New Brunswick. Atl Geol 38:29–36

Montel JM (1993) A model for monazite/melt equilibrium and application to the generation of granitic magmas. Chem Geol 110:127–146

Müller D, Groves DI (1993) Direct and indirect associations between potassic igneous rocks, shaoshonites and gold-copper deposits. Ore Geol Rev 8:383–406

Müller D, Groves DI (2000) Potassic igneous rocks and associated gold-copper mineralization. Springer, Berlin Heidelberg New York, 252 pp

Munoz JL (1984) F-OH and Cl-OH exchange in micas with application to hydrothermal systems. In: Bailey SW (ed) Micas. Rev Mineral 13:469–494

Munoz JL (1992) Calculation of HF and HCl fugacities from biotite compositions: revised equations. Geological Society of American, Abstracts with Programs 24:221

Munoz JL, Swenson A (1981) Chloride-hydroxyl exchange in biotite and estimation of relative HCl/HF activities in hydrothermal fluids. Econ Geol 76:2212–2221

Piccoli PM, Candela PA, Williams TJ (1999) Estimation of aqueous HCl and Cl concentrations in felsic systems. Lithos 46:591–604

Poli S, Schmidt MW (1992) A comment on ''Calcic amphibole equilibria and a new amphibole-plagioclase geothermometer'' by Blundy JD and Holland TJB (Contrib Mineral Petrol, 1990, 104:208–224). Contrib Mineral Petrol 111:273–278

Richards JP (1995) Alkalic-type epithermal gold deposits—a review. In: Thompson JFH (ed) Magmas, fluids, and ore deposits. Mineralogical Association of Canada Short course, Series vol 23, pp 367–400

Rieder M, Cavazzini G, D'Yakonov YS, Frank-Kamenetskii VA, Gottardi G, Guoggenheim S, Koval PV, Müller G, Neiva AMR, Radoslovich EW, Robert J-L, Sssi FP, Takeda H, Weiss Z, Wones DR (1998) Nomenclature of the micas. Can Mineral 36:905–912

Righter K, Dyar MD, Delaney JS, Vennemann TW, Hervig RL, King PL (2002) Correlations of octahedral cations with OH^-, O^{2-}, Cl^-, and F^- in biotite from volcanic rocks and xenoliths. Am Mineral 87:142–153

Rutherford MJ, Johnson MC (1992) Comment on Blundy and Holland's (1990) ''Calcic amphibole equilibria and a new amphibole-plagioclase geothermometer''. Contrib Mineral Petrol 111:266–268

Rutter MJ, Van der Laan SR, Wyllie PJ (1989) Experimental data for a proposed empirical igneous geobarometer: aluminum in hornblende at 10 kbar pressure. Geology 17:897–900

Scaillet B, Holtz F, Pichavant M (1998) Phase equilibrium constraints on the viscosity of silicic magmas. 1. Volcanic–plutonic comparison. J Geophys Res 103:27257–27266

Seal RR II, Clark AH, Morrissy CJ (1987) Stockwork tungsten (scheelite)-molybdenum mineralization, Lake George, southwestern New Brunswick. Econ Geol 82:1259–1282

Shabani AAT, Lalonde A, Whalen JB (2003) Composition of biotite from granitic rocks of the Canadian Appalachian orogen: a potential tectonomagmatic indicator? Can Mineral 41:1381–1396

Shaw CSJ, Penczak RP (1996) Barium-rich biotite and phlogopite from the Western and Eastern Gabbro, Coldwell alkaline complex, northwest Ontario.Can Mineral 34:967–975

Sinclair WD, Kooiman GJA, Martin DA (1988) Geological setting of granites and related tin deposits in the North Zone, Mount Pleasant, New Brunswick. Geological Survey of Canada, Current Research, Part B, Paper 88–1B, pp 201–208

Speer JA (1984) Micas in igneous rocks. In: Bailey SW (ed) Micas. Rev Mineral 13:299–356

Stein E, Dietl C (2001) Hornblende thermobarometry of granitoids from the Central Odenwald (Germany) and their implications for the geotectonic development of the Odenwald. Mineral Petrol 72:185–207

Stormer JC Jr (1975) A practical two-feldspar geothermometer. Am Mineral 60:667–674

Taylor RP (1992) Petrological and geochemical characteristics of the Pleasant Ridge zinnwaldite topaz granite, southern New Brunswick, and comparisons with other topaz-bearing felsic rocks. Can Mineral 30:895–921

Thompson AB (2001) Clockwise P–T paths for crustal melting and H_2O recycling in granite source regions and migmatite terrains. Lithos 56:33–45

Thompson JFH, Newberry RJ (2000) Gold deposits related to reduced granitic intrusions. Rev Econ Geol 13:377–400

Thompson JFH, Sillitoe RH, Baker T, Lang GJR, Mortensen JK (1999) Intrusion-related gold deposits associated with tungsten tin provinces. Mineralium Deposita 34:323–334

Thorne KG, Lentz DR, Hall DC, Yang xm (2002) Petrology, geochemistry, and geochronology of the granitic pegmatite and aplite dykes associated with the Clarence Stream gold deposit, southwestern New Brunswick. Geological Survey of Canada, Current Research 2002-E12:1–13

Watson EB, Harrison TM (1983) Zircon saturation revisited: temperature and composition effects in a variety of crustal magma types. Earth Planet Sci Lett 64:295–304

Whalen JB (1993) Geology, petrography, and geochemistry of Appalachian granites in New Brunswick and Gaspésie, Quebec. Geological Survey of Canada Bulletin 436, 124 pp

Whalen JB, Fyffe LR, Longstaffe FJ, Jenner GA (1996) The position and nature of the Gander Avalon boundary, southern New Brunswick, based on geochemical and isotopic data from granitoid rocks. Can J Earth Sci 33:129–139

Whitney JA (1988) The origin of granite: the role and source of water in the evolution of granitic magmas. Geol Soc Am Bull 100:1886–1897

Williams H, Dehler SA, Grant AC, Oakey GN (1999) Tectonics of Atlantic Canada. Geosci Can 26:51–70

Wones DR (1980) Contributions of crystallography, mineralogy, and petrology to the geology of the Lucerne pluton, Hancock County, Maine. Am Mineral 65:411–437

Wones DR (1989) Significance of the assemblage titanite + magnetite + quartz in granitic rocks. Am Mineral 74:744–749

Wones DR, Eugster HP (1965) Stability of biotite: experiment, theory, and application. Am Mineral 50:1228–1272

Wyllie PJ (1977) Crustal anatexis: an experimental review. Tectonophysics 43:41–71

Yang XM, Lentz DR, Chi G (2002a) Petrochemistry of Lake George granodiorite stock and related Au mineralization, York County, New Brunswick. Geological Survey of Canada, Current Research 2002-D7:1–10

Yang XM, Lentz DR, Hall DC, Chi G (2002b) Petrology of the Lake George granodiorite stock, New Brunswick: implications for crystallization conditions, volatile exsolution, and W-Mo-Au-Sb mineralization. Geological Survey of Canada, Current Research 2002-E14:1–12

Yang XM, Lentz DR, McCutcheon SR (2003) Petrochemical evolution of subvolcanic granitoid intrusions within the Late Devonian Mount Pleasant Caldera, southwestern New Brunswick, Canada: comparison of Au versus Sn-W-Mo-polymetallic mineralization systems. Atl Geol 39:97–121

Yang XM, Lentz DR, Chi G, Kyser TK (2004a) Fluid-mineral reaction in the Lake George granodiorite, New Brunswick: implications for Au-W-Mo-Sb mineralization. Can Mineral 42:1443–1464

Yang XM, Lentz DR, Chi G, Thorne KG (2004b) Petrochemical characteristics of gold-related granitoids in southwestern New Brunswick, Canada. Exploration and Mining Geology (in press)

Zhu C, Sverjensky DA (1991) Partitioning of F-Cl-OH between minerals and hydrothermal fluids. Geochimica Cosmochimica Acta 55:1837–1858